

Periodic thermodynamics of the Rabi model with circular polarization for arbitrary spin quantum numbers

Heinz-Jürgen Schmidt¹, Jürgen Schnack², and Martin Holthaus³

¹*Universität Osnabrück, Fachbereich Physik, D-49069 Osnabrück, Germany*

²*Universität Bielefeld, Fakultät für Physik, D-33501 Bielefeld, Germany and*

³*Carl von Ossietzky Universität, Institut für Physik, D-26111 Oldenburg, Germany*

We consider a spin s subjected to both a static and an orthogonally applied oscillating, circularly polarized magnetic field while being coupled to a heat bath, and analytically determine the quasistationary distribution of its Floquet-state occupation probabilities for arbitrarily strong driving. This distribution is shown to be Boltzmannian with a quasitemperature which is different from the temperature of the bath, and independent of the spin quantum number. We discover a remarkable formal analogy between the quasithermal magnetism of the nonequilibrium steady state of a driven ideal paramagnetic material, and the usual thermal paramagnetism. Nonetheless, the response of such a material to the combined fields is predicted to show several unexpected features, even allowing one to turn a paramagnet into a diamagnet under strong driving. Thus, we argue that experimental measurements of this response may provide key paradigms for the emerging field of periodic thermodynamics.

Keywords: Periodically driven quantum systems, Rabi problem, Floquet states, quasistationary distribution, quasitemperature, nonequilibrium steady state, paramagnetism

I. INTRODUCTION

A quantum system governed by an explicitly time-dependent Hamiltonian $H(t)$ which varies *periodically* with time t , such that

$$H(t) = H(t + T), \quad (1)$$

possesses a complete set of *Floquet states*, that is, of solutions to the time-dependent Schrödinger equation having the particular form

$$|\psi_n(t)\rangle = |u_n(t)\rangle \exp(-i\varepsilon_n t). \quad (2)$$

The *Floquet functions* $|u_n(t)\rangle$ share the T -periodic time dependence of their Hamiltonian,

$$|u_n(t)\rangle = |u_n(t + T)\rangle; \quad (3)$$

the quantities ε_n , which accompany their time evolution in the same manner as energy eigenvalues accompany the evolution of unperturbed energy eigenstates, are known as *quasienergies* [1–3]. Here we assume that the quasienergies constitute a pure point spectrum, associated with square-integrable Floquet states in the system's Hilbert space \mathcal{H}_S ; we also adopt a system of units such that both the Planck constant \hbar and the Boltzmann constant k_B are set to one.

Evidently the factorization of a Floquet state (2) into a Floquet function and an exponential of a phase which grows linearly in time is not unique: Defining $\omega = 2\pi/T$, and taking an arbitrary, positive or negative integer ν , one has

$$|u_n(t)\rangle \exp(-i\varepsilon_n t) = |u_n(t)e^{i\nu\omega t}\rangle \exp(-i[\varepsilon_n + \nu\omega]t), \quad (4)$$

where $|u_n(t)e^{i\nu\omega t}\rangle$ again is a T -periodic Floquet function, representing the same Floquet state as $|u_n(t)\rangle$. Therefore, a quasienergy is not to be regarded as just a single number equipped with the dimension of energy, but

rather as an infinite set of equivalent representatives,

$$[\varepsilon_n] \equiv \{\varepsilon_n + \nu\omega \mid \nu \in \mathbb{Z}\}, \quad (5)$$

where the choice of the “canonical representative” distinguished by setting $\nu = 0$ is a matter of convention.

The significance of these Floquet states (2) rests in the fact that, as long as the Hamiltonian depends on time in a strictly T -periodic manner, every solution $|\psi(t)\rangle$ to the time-dependent Schrödinger equation can be expanded with respect to the Floquet basis,

$$|\psi(t)\rangle = \sum_n c_n |u_n(t)\rangle \exp(-i\varepsilon_n t), \quad (6)$$

where the coefficients c_n do not depend on time. Hence, the Floquet states propagate with constant occupation probabilities $|c_n|^2$, despite the presence of a time-periodic drive. Under conditions of perfectly coherent time evolution these coefficients c_n would be determined solely by the system's state at the moment the periodic drive is turned on. However, if the periodically driven system is interacting with an environment, as it happens in many cases of experimental interest [4–9], that environment may continuously induce transitions among the system's Floquet states, to the effect that a quasistationary distribution $\{p_n\}$ of Floquet-state occupation probabilities establishes itself which contains no memory of the initial state, and the question emerges how to quantify this distribution.

In a short programmatic note entitled “Periodic Thermodynamics”, Kohn has drawn attention to such quasistationary Floquet-state distributions $\{p_n\}$, emphasizing that they should be less universal than usual distributions characterizing thermal equilibrium, depending on the very form of the system's interaction with its environment [10]. In an earlier pioneering study, Breuer *et*

al. had already calculated these distributions for time-periodically forced oscillators coupled to a thermal oscillator bath [11]. For the particular case of a linearly forced *harmonic* oscillator these authors have shown that the Floquet-state distribution remains a Boltzmann distribution parametrized by the temperature of the heat bath, whereas it becomes rather more complicated in the case of forced *anharmonic* oscillators. These investigations have been extended later by Ketzmerick and Wustmann, who have demonstrated that structures found in the phase space of classical forced anharmonic oscillators leave their distinct traces in the quasistationary Floquet-state distributions of their quantum counterparts [12]. To date, a great variety of different individual aspects of the “periodic thermodynamics” envisioned by Kohn has been discussed in the literature [13–24], but a coherent overall picture is still lacking.

In this situation it seems advisable to resort to models which are sufficiently simple to admit analytical solutions and thus to unravel salient features on the one hand, and which actually open up meaningful perspectives for groundbreaking novel laboratory experiments on the other. To this end, in the present work we consider a spin s exposed to both a static magnetic field and an oscillating, circularly polarized magnetic field applied perpendicularly to the static one, as in the classic Rabi setup [25], and coupled to a thermal bath of harmonic oscillators. The experimental measurement of the thermal paramagnetism resulting from magnetic moments subjected to a static field alone has a long and successful history [26, 27], having become a standard topic in textbooks on Statistical Physics [28, 29]. We argue that a future generation of such experiments, including both a static and a strong oscillating field, may set further milestones towards the development of full-fledged periodic thermodynamics.

We proceed as follows: In Sec. II we collect the necessary technical tools, starting with a brief summary of the golden-rule approach to time-periodically driven open quantum systems in the form developed by Breuer *et al.* [11], thereby establishing our notation. We also sketch a technique which enables one to “lift” a solution to the Schrödinger equation for a spin $s = 1/2$ in a time-varying magnetic field to general s . In Sec. III we discuss the Floquet states for spins in a circularly polarized driving field, obtaining the states for general s from those for $s = 1/2$ with the help of the lifting procedure. In Sec. IV we compute the quasistationary Floquet-state distribution for driven spins under the assumption that the spectral density of the heat bath be constant, and show that this distribution is Boltzmannian with a quasitemperature which is *different* from the actual bath temperature; the dependence of this quasitemperature on the system parameters is discussed in some detail. In Sec. V we determine the magnetization of a spin system which is subjected to both a static and an orthogonally applied, circularly polarized magnetic field while being coupled to a heat bath. To this end, we first establish a general

formula for the ensuing magnetization by means of another systematic use of the lifting technique, and then show that the resulting expression can be interpreted as a derivative of a partition function based on both the quasitemperature and the system’s quasienergies, in perfect formal analogy to the textbook treatment of paramagnetism in the absence of time-periodic driving; these insights are exploited for elucidating the response of an ideal paramagnet to a circularly polarized driving field. In Sec. VI we consider the rate of energy dissipated by the driven spins into the bath, thus generalizing results derived previously for $s = 1/2$ in Ref. [30]. In Sec. VII we summarize and discuss our main findings, emphasizing the possible knowledge gain to be derived from future measurements of paramagnetic response to strong time-periodic forcing, carried out along the lines drawn in the present work.

II. TECHNICAL TOOLS

A. Golden-rule approach to open driven systems

Let us consider a quantum system evolving according to a T -periodic Hamiltonian $H(t)$ on a Hilbert space \mathcal{H}_S which is perturbed by a time-independent operator V . Then the transition matrix element connecting an initial Floquet function $|u_i(t)\rangle$ to a final Floquet function $|u_f(t)\rangle$ can be expanded into a Fourier series,

$$\langle u_f(t) | V | u_i(t) \rangle = \sum_{\ell \in \mathbb{Z}} V_{fi}^{(\ell)} \exp(i\ell\omega t), \quad (7)$$

and consequently the “golden rule” for the rate of transitions Γ_{fi} from a Floquet state labeled i to a Floquet state f is written as [30]

$$\Gamma_{fi} = 2\pi \sum_{\ell \in \mathbb{Z}} |V_{fi}^{(\ell)}|^2 \delta(\omega_{fi}^{(\ell)}), \quad (8)$$

where

$$\omega_{fi}^{(\ell)} = \varepsilon_f - \varepsilon_i + \ell\omega. \quad (9)$$

Thus, a transition among Floquet states is not simply associated with only one single frequency, but rather with a set of frequencies spaced by integer multiples of the driving frequency ω , reflecting the ladder-like nature of the system’s quasienergies (5); this is one of the sources of the peculiarities which distinguish periodic thermodynamics from usual equilibrium thermodynamics [10, 11].

Let us now assume that, instead of merely being perturbed by V , the periodically driven system is coupled to a heat bath, described by a Hamiltonian H_{bath} acting on a Hilbert space \mathcal{H}_B , so that the total Hamiltonian on the composite Hilbert space $\mathcal{H}_S \otimes \mathcal{H}_B$ takes the form

$$H_{\text{total}}(t) = H(t) \otimes \mathbb{1} + \mathbb{1} \otimes H_{\text{bath}} + H_{\text{int}}. \quad (10)$$

Stipulating further that the interaction Hamiltonian H_{int} factorizes according to

$$H_{\text{int}} = V \otimes W, \quad (11)$$

the golden rule can be applied to joint transitions from Floquet states i to Floquet states f of the system accompanied by transitions from bath eigenstates n with energy E_n to other bath eigenstates m with energy E_m , acquiring the form

$$\Gamma_{fi}^{mn} = 2\pi \sum_{\ell \in \mathbb{Z}} |V_{fi}^{(\ell)}|^2 |W_{mn}|^2 \delta(E_m - E_n + \omega_{fi}^{(\ell)}). \quad (12)$$

Moreover, following Breuer *et al.* [11], let us consider a bath consisting of thermally occupied harmonic oscillators, and an interaction of the prototypical form

$$W = \sum_{\tilde{\omega}} \left(b_{\tilde{\omega}} + b_{\tilde{\omega}}^{\dagger} \right), \quad (13)$$

where $b_{\tilde{\omega}}$ ($b_{\tilde{\omega}}^{\dagger}$) is the annihilation (creation) operator pertaining to a bath oscillator of frequency $\tilde{\omega}$. One could also multiply W by a function $g(\tilde{\omega})$ specifying a frequency-dependent coupling strength, but this function could be absorbed in the spectral density of the bath introduced later, and therefore will not be used here.

We now have to distinguish two cases: If $E_n - E_m = \tilde{\omega} > 0$, so that the bath is de-excited and transfers energy to the system, the required annihilation-operator matrix element reads

$$W_{mn} = \sqrt{n(\tilde{\omega})}, \quad (14)$$

where $n(\tilde{\omega})$ is the occupation number of a bath oscillator with frequency $\tilde{\omega}$, and the square $|W_{mn}|^2$ entering the golden rule (12) has to be replaced by the thermal average

$$N(\tilde{\omega}) \equiv \langle n(\tilde{\omega}) \rangle = \frac{1}{\exp(\beta\tilde{\omega}) - 1}, \quad (15)$$

with β denoting the inverse bath temperature. Conversely, if $E_n - E_m = \tilde{\omega} < 0$ so that the system loses energy to the bath and a bath phonon is created, one has

$$W_{mn} = \sqrt{n(-\tilde{\omega}) + 1}, \quad (16)$$

giving

$$N(\tilde{\omega}) \equiv \langle n(-\tilde{\omega}) \rangle + 1 = \frac{1}{1 - \exp(\beta\tilde{\omega})}. \quad (17)$$

Finally, let $J(\tilde{\omega})$ be the spectral density of the bath. Then the total rate Γ_{fi} of bath-induced transitions among the Floquet states i and f of the driven system is expressed as a sum of partial rates,

$$\Gamma_{fi} = \sum_{\ell \in \mathbb{Z}} \Gamma_{fi}^{(\ell)}, \quad (18)$$

where

$$\Gamma_{fi}^{(\ell)} = 2\pi |V_{fi}^{(\ell)}|^2 N(\omega_{fi}^{(\ell)}) J(|\omega_{fi}^{(\ell)}|). \quad (19)$$

The evaluation of this formula requires a definite specification of the quasienergy representatives for each state when computing the transition frequencies (9); this specification also fixes the representatives of the Floquet functions which enter the matrix elements (7). An alternative choice of representatives would lead to a shift of the Fourier index ℓ , but leaves the sum (18) invariant.

These total rates (18) now determine the desired quasi-stationary distribution $\{p_n\}$ as a solution to the equation [11]

$$\sum_m (\Gamma_{nm} p_m - \Gamma_{mn} p_n) = 0. \quad (20)$$

It deserves to be emphasized again that the very details of the system-bath coupling enter here, so that the precise form of the respective distribution $\{p_n\}$ may depend strongly on such details [10].

B. The lift from $s = 1/2$ to general s

We will make heavy use of a procedure which allows one to transfer a solution to the Schrödinger equation for a spin with spin quantum number $s = 1/2$ in a time-dependent external field to a solution of the corresponding Schrödinger equation for general s , see also Ref. [31]. This procedure essentially rests on the fact that a spin- s state can be represented as a direct symmetrized product of $2s$ spin-1/2 states, as exposed by Landau and Lifshitz [32]. It does not appear to be widely known, but has been applied already in 1987 to the coherent evolution of a laser-driven N -level system possessing an $SU(2)$ dynamic symmetry [33], and more recently to the spin- s Landau-Zener problem [34]. Here we briefly sketch this method.

Let $t \mapsto \Psi(t) \in SU(2)$ be a smooth curve such that $\Psi(0) = 1$, as given by a 2×2 -matrix of the form

$$\Psi(t) = \begin{pmatrix} z_1(t) & z_2(t) \\ -z_2^*(t) & z_1^*(t) \end{pmatrix} \quad (21)$$

with complex functions $z_1(t)$, $z_2(t)$ obeying $|z_1(t)|^2 + |z_2(t)|^2 = 1$ for all times t . One then has

$$\left(\frac{d}{dt} \Psi(t) \right) \Psi(t)^{-1} \equiv -iH(t) \in su(2), \quad (22)$$

where $su(2)$ denotes the Lie algebra of $SU(2)$, *i.e.*, the space of anti-Hermitian, traceless 2×2 -matrices which is closed under commutation [35]. Hence the columns $|\psi_1(t)\rangle$, $|\psi_2(t)\rangle$ of $\Psi(t)$ are linearly independent solutions of the Schrödinger equation

$$i \frac{d}{dt} |\psi_j(t)\rangle = H(t) |\psi_j(t)\rangle, \quad j = 1, 2. \quad (23)$$

Next we consider the well-known irreducible Lie algebra representation of $su(2)$,

$$r^{(s)} : su(2) \longrightarrow su(2s+1) , \quad (24)$$

which is parametrized by a spin quantum number s such that $2s \in \mathbb{N}$, together with the corresponding irreducible group representation (“irrep” for brevity)

$$R^{(s)} : SU(2) \longrightarrow SU(2s+1) . \quad (25)$$

One then has [35]

$$r^{(s)}(is_j) = iS_j , \quad j = x, y, z , \quad (26)$$

where $s_j = \sigma_j/2$ denote the three $s = 1/2$ spin operators given by the Pauli matrices σ_j , and the S_j denote the corresponding spin operators for general s . Recall the standard matrices

$$\begin{aligned} (S_z)_{m,n} &= n \delta_{m,n} , \\ (S_x)_{m,n} &= \begin{cases} \frac{1}{2} \sqrt{s(s+1) - n(n \pm 1)} & : m = n \pm 1 , \\ 0 & : \text{else} , \end{cases} \\ (S_y)_{m,n} &= \begin{cases} \pm \frac{1}{2i} \sqrt{s(s+1) - n(n \pm 1)} & : m = n \pm 1 , \\ 0 & : \text{else} , \end{cases} \end{aligned} \quad (27)$$

where $m, n = s, s-1, \dots, -s$, and

$$S_{\pm} \equiv S_x \pm iS_y . \quad (28)$$

It follows from the general theory of representations [35] that $r^{(s)}$ and $R^{(s)}$ may be applied to Eq. (22) and yield

$$\left(\frac{d}{dt} R^{(s)} \Psi(t) \right) \left(R^{(s)} \Psi(t) \right)^{-1} = r^{(s)}(-iH(t)) . \quad (29)$$

Since the traceless matrix $H(t)$ can always be written as a linear combination of the spin operators s_j it acquires the form of a Zeeman term with a time-dependent magnetic field $\mathbf{b}(t)$, namely,

$$H(t) = \mathbf{b}(t) \cdot \mathbf{s} = \sum_{j=1}^3 b_j(t) s_j , \quad (30)$$

and Eq. (26) now implies

$$r^{(s)}(-iH(t)) = -i \mathbf{b}(t) \cdot \mathbf{S} = -i \sum_{j=1}^3 b_j(t) S_j . \quad (31)$$

Hence, the “lifted” matrix

$$\Psi^{(s)}(t) \equiv R^{(s)}(\Psi(t)) \quad (32)$$

will be a matrix solution to the lifted Schrödinger equation

$$i \frac{d}{dt} \Psi^{(s)}(t) = \mathbf{b}(t) \cdot \mathbf{S} \Psi^{(s)}(t) . \quad (33)$$

Note that the matrix $\Psi^{(s)}(t)$ is unitary, and hence its columns span the general $(2s+1)$ -dimensional solution space of the lifted Schrödinger equation (33). The decisive step of this procedure, namely, the lift from Eq. (22) to Eq. (29), is further illustrated in Appendix A with the help of an elementary example.

III. FLOQUET FORMULATION OF THE RABI PROBLEM

A. Floquet decomposition for $s = 1/2$

A spin $1/2$ subjected to both a constant magnetic field applied in the z -direction and an orthogonal, circularly polarized time-periodic field, as constituting the classic Rabi problem [25], is described by the Hamiltonian

$$H(t) = \frac{\omega_0}{2} \sigma_z + \frac{F}{2} (\sigma_x \cos \omega t + \sigma_y \sin \omega t) . \quad (34)$$

Here $\omega_0 > 0$ denotes the transition frequency pertaining to the spin states in the static field alone, while F , carrying the dimension of a frequency in our system of units, denotes the amplitude of the periodic drive. This is a special form of the Zeeman Hamiltonian (30) with the particular choices

$$\begin{aligned} b_x(t) &= F \cos \omega t \\ b_y(t) &= F \sin \omega t \\ b_z(t) &= \omega_0 . \end{aligned} \quad (35)$$

The Floquet states (2) brought about by this Hamiltonian (34) are given by [36]

$$|\psi_{\pm}(t)\rangle = \frac{e^{\mp i\Omega t/2}}{\sqrt{2\Omega}} \begin{pmatrix} \pm \sqrt{\Omega \pm \delta} e^{-i\omega t/2} \\ \sqrt{\Omega \mp \delta} e^{+i\omega t/2} \end{pmatrix} , \quad (36)$$

where

$$\delta = \omega_0 - \omega \quad (37)$$

denotes the detuning of the transition frequency ω_0 from the driving frequency ω , and Ω is the Rabi frequency,

$$\Omega = \sqrt{\delta^2 + F^2} . \quad (38)$$

The 2×2 -matrix $\Psi(t)$ constructed from these states does not satisfy $\Psi(0) = \mathbb{1}$. This is of no concern, since $\Psi(t)$ could be replaced by $\Psi(t)(\Psi(0))^{-1}$. The distinct advantage of these Floquet solutions (36) lies in the fact that they yield a particularly convenient starting point for the lifting procedure outlined in Sec. II B: One has

$$\begin{aligned} \Psi(t) &= \frac{1}{\sqrt{2\Omega}} \begin{pmatrix} \sqrt{\Omega + \delta} & -\sqrt{\Omega - \delta} \\ e^{i\omega t} \sqrt{\Omega - \delta} & e^{i\omega t} \sqrt{\Omega + \delta} \end{pmatrix} \\ &\quad \times \begin{pmatrix} e^{-i(\omega + \Omega)t/2} & 0 \\ 0 & e^{-i(\omega - \Omega)t/2} \end{pmatrix} \\ &\equiv P(t) e^{-i\omega t/2} \exp(-i\Omega t s_z) . \end{aligned} \quad (39)$$

This decomposition possesses the general Floquet form

$$\Psi(t) = P(t) \exp(-iGt) , \quad (40)$$

where the unitary matrix $P(t) = P(t+T)$ again is T -periodic, and the eigenvalues of the “Floquet matrix” G , to be obtained from the matrix logarithm

of $\Psi(T)(\Psi(0))^{-1} = \exp(-iGT)$, provide the system's quasienergies [37–40]. Since G already is diagonal in this representation (39), the quasienergies of a spin 1/2 driven by a circularly polarized field according to the Hamiltonian (34) can be read off immediately:

$$\varepsilon_{\pm} = \frac{\omega \pm \Omega}{2} \mod \omega, \quad (41)$$

satisfying $\varepsilon_+ + \varepsilon_- = 0 \mod \omega$. For later application we express the periodic part $P(t)$ of the decomposition (39) in the following way:

$$\begin{aligned} P(t) &= e^{i\omega t/2} \begin{pmatrix} e^{-i\omega t/2} & 0 \\ 0 & e^{+i\omega t/2} \end{pmatrix} \\ &\quad \times \frac{1}{\sqrt{2\Omega}} \begin{pmatrix} \sqrt{\Omega + \delta} & -\sqrt{\Omega - \delta} \\ \sqrt{\Omega - \delta} & \sqrt{\Omega + \delta} \end{pmatrix} \\ &\equiv e^{i\omega t/2} \exp(-i\omega t s_z) \Xi. \end{aligned} \quad (42)$$

The time-independent matrix $\Xi = \Psi(0)$ introduced here can be written as

$$\Xi = \exp(-i\lambda s_y) = \begin{pmatrix} \cos(\lambda/2) & -\sin(\lambda/2) \\ \sin(\lambda/2) & \cos(\lambda/2) \end{pmatrix} \quad (43)$$

with

$$\lambda/2 = \arccos \left(\sqrt{\frac{\Omega + \delta}{2\Omega}} \right). \quad (44)$$

Hence, one has the identities

$$\begin{aligned} \Xi^\dagger s_x \Xi &= \frac{\delta}{\Omega} s_x + \frac{\sqrt{\Omega^2 - \delta^2}}{\Omega} s_z \\ \Xi^\dagger s_y \Xi &= s_y, \\ \Xi^\dagger s_z \Xi &= \frac{\delta}{\Omega} s_z - \frac{\sqrt{\Omega^2 - \delta^2}}{\Omega} s_x, \end{aligned} \quad (45)$$

which will be put into use in both Sec. IV and Sec. V.

B. Floquet decomposition for general s

Replacing the spin-1/2 operators $s_j = \sigma_j/2$ in the Hamiltonian (34) by their counterparts S_j for general spin quantum number s , one obtains

$$\begin{aligned} H^{(s)}(t) &= \mathbf{b}(t) \cdot \mathbf{S} \\ &= \omega_0 S_z + F (S_x \cos \omega t + S_y \sin \omega t). \end{aligned} \quad (46)$$

According to Sec. IIB the general matrix solution to the corresponding Schrödinger equation (33) now is obtained as the lift (32) of the 2×2 -matrix (39). Invoking Eqs. (42) and (43), and applying the irrep $R^{(s)}$ to this decomposition yields

$$\begin{aligned} \Psi^{(s)}(t) &= R^{(s)} \left(\exp(-i\omega t s_z) \exp(-i\lambda s_y) \exp(-i\Omega t s_z) \right) \\ &= \exp(-i\omega t S_z) \exp(-i\lambda S_y) \exp(-i\Omega t S_z). \end{aligned} \quad (47)$$

In order to bring this factorization into the standard Floquet form analogous to Eq. (40),

$$\Psi^{(s)}(t) = P^{(s)}(t) \exp(-iG^{(s)}t) \quad (48)$$

with a T -periodic matrix $P^{(s)}(t) = P^{(s)}(t + T)$, we have to distinguish two cases:

(i) For *integer* s we may set

$$\begin{aligned} P^{(s)}(t) &= \exp(-i\omega t S_z) \exp(-i\lambda S_y), \\ G^{(s)} &= \Omega S_z. \end{aligned} \quad (49)$$

(ii) For *half-integer* s the requirement that $P^{(s)}(t)$ be T -periodic demands insertion of additional factors $e^{\pm i\omega t/2}$, in analogy to the representation (42) for $s = 1/2$. This gives

$$\begin{aligned} P^{(s)}(t) &= e^{i\omega t/2} \exp(-i\omega t S_z) \exp(-i\lambda S_y), \\ G^{(s)} &= \frac{\omega}{2} \mathbb{1}^{(s)} + \Omega S_z, \end{aligned} \quad (50)$$

where $\mathbb{1}^{(s)}$ indicates the unit matrix in \mathbb{C}^{2s+1} .

Denoting the eigenstates of S_z as $|m\rangle$, such that $S_z|m\rangle = m|m\rangle$, we now introduce Floquet functions and their quasienergies according to the prescription

$$\begin{aligned} \Psi^{(s)}(t) |m\rangle &= P^{(s)}(t) |m\rangle \exp(-i\varepsilon_m t) \\ &\equiv |u_m(t)\rangle \exp(-i\varepsilon_m t), \end{aligned} \quad (51)$$

implying the particular choice

$$|u_m(t)\rangle = P^{(s)}(t) |m\rangle \quad (52)$$

of T -periodic Floquet functions. The associated quasi-energy representatives then are

$$\varepsilon_m = m\Omega \quad (53)$$

for integer s according to case (i), or

$$\varepsilon_m = \frac{\omega}{2} + m\Omega \quad (54)$$

for half-integer s according to case (ii), with $m = -s, \dots, s$. This convenient choice of representatives will be presupposed in the following for computing the partial rates (19). Observe that there is a further, physically important distinction to be made at this point: When the driving amplitude vanishes, that is, for $F \rightarrow 0$, the Rabi frequency (38) does not reduce to the detuning, but rather to the absolute value of the detuning, $\Omega \rightarrow |\omega_0 - \omega|$. Hence, for $F \rightarrow 0$ the Floquet functions (52) “connect” to $|m\rangle$ only for red detuning, when $\omega < \omega_0$, but to $|-m\rangle$ for blue detuning, when $\omega > \omega_0$. Hence, under blue detuning the labeling of the Floquet functions and their quasienergies effectively is reversed with respect to the eigenstates of S_z . This feature needs to be kept in mind for correctly assessing the following results.

We also note that in the adiabatic low-frequency limit, when the spin is exposed to an arbitrarily slowly varying magnetic field enabling adiabatic following to the instantaneous energy eigenstates, the quasienergies should be given by the one-cycle averages of the instantaneous energy eigenvalues. Indeed, in this limit the Rabi frequency (38) reduces to $\Omega = \sqrt{\omega_0^2 + F^2}$, while the time-independent instantaneous energy levels are $E_m = m\Omega$, yielding the expected identity.

IV. THE QUASISTATIONARY DISTRIBUTION

Now we stipulate that the periodically driven spin be coupled to a thermal bath of harmonic oscillators, as sketched in Sec. II A, taking the coupling operator to be of the simple form [41]

$$V = \gamma S_x. \quad (55)$$

In order to calculate the Fourier decompositions (7) of the Floquet matrix elements of V , and referring to the above representation (52) of the Floquet functions, we thus need to consider the operator

$$\begin{aligned} & P^{(s)\dagger}(t) S_x P^{(s)}(t) \\ &= \exp(i\lambda S_y) \exp(i\omega t S_z) S_x \exp(-i\omega t S_z) \exp(-i\lambda S_y) \\ &\equiv \sum_{\ell \in \mathbb{Z}} V^{(\ell)} \exp(i\ell\omega t); \end{aligned} \quad (56)$$

note that the additional phase factor $e^{i\omega t/2}$ contained in the expression (50) for $P^{(s)}(t)$ with half-integer s cancels here. Using the $su(2)$ commutation relations and their counterparts for general s , we deduce

$$\begin{aligned} & \exp(i\omega t S_z) S_x \exp(-i\omega t S_z) \\ &= \frac{1}{2} (e^{i\omega t} S_+ + e^{-i\omega t} S_-). \end{aligned} \quad (57)$$

Hence, as in the case $s = 1/2$ studied in Ref. [30], the only non-vanishing Fourier components $V^{(\ell)}$ occur for $\ell = \pm 1$:

$$V^{(\pm 1)} = \frac{\gamma}{2} \exp(i\lambda S_y) S_{\pm} \exp(-i\lambda S_y). \quad (58)$$

Applying $R^{(s)}$ to Eqs. (45), this yields

$$V^{(\pm 1)} = \frac{\gamma}{2} \left(\frac{\delta}{\Omega} S_x + \frac{\sqrt{\Omega^2 - \delta^2}}{\Omega} S_z \pm i S_y \right). \quad (59)$$

Thus, $V^{(\pm 1)}$ is a tridiagonal matrix. For computing the partial transition rates (19) we therefore have to consider only frequencies $\omega_{mn}^{(\pm 1)}$ of pseudotransitions [30], for which $m = n$, and of transitions between neighboring Floquet states, $m = n \pm 1$. For evaluating the definition (9) one now has to resort to the quasienergy representatives (53) and (54) which belong to the Floquet functions (52) entering here, giving

$$\omega_{mn}^{(\pm 1)} = \begin{cases} \pm\omega & : m = n, \\ \Omega \pm \omega & : m = n + 1, \\ -\Omega \pm \omega & : m = n - 1. \end{cases} \quad (60)$$

According to the Pauli master equation (20), the quasistationary distribution $\{p_m\}_{m=s, \dots, -s}$ which establishes itself under the combined influence of time-periodic driving and the thermal oscillator bath is the eigenvector of a tridiagonal matrix $\tilde{\Gamma}$ corresponding to the eigenvalue 0, where $\tilde{\Gamma}$ is obtained from $\Gamma \equiv \Gamma^{(1)} + \Gamma^{(-1)}$ by subtracting from the diagonal elements the respective column sums, *i.e.*,

$$\tilde{\Gamma}_{mn} = \Gamma_{mn} - \delta_{mn} \sum_{k=-s}^s \Gamma_{kn}. \quad (61)$$

Since $\tilde{\Gamma}$ is tridiagonal with non-vanishing secondary diagonal elements, this eigenvector is unique up to normalization. Moreover, it is evident that we only need the matrix elements of Γ in the secondary diagonals for calculating the quasistationary distribution, whereas the diagonal elements will be required for computing the dissipation rate [30].

The very fact that $V^{(\pm 1)}$, and hence Γ , merely is a tridiagonal matrix has a conceptually important consequence: It enforces detailed balance, meaning that each term of the sum (20) vanishes individually. With Γ being tridiagonal, this sum reduces to

$$\begin{aligned} & (\Gamma_{n,n-1} p_{n-1} - \Gamma_{n-1,n} p_n) \\ & + (\Gamma_{n,n+1} p_{n+1} - \Gamma_{n+1,n} p_n) = 0 \end{aligned} \quad (62)$$

for all $n = -s + 1, \dots, s - 1$, since the term with $m = n$ in Eq. (20) cancels. In the border cases $n = -s$ or $n = s$ this identity still holds, but only one bracket survives. Upon setting the first bracket in this Eq. (62) to zero, one obtains

$$\frac{p_n}{p_{n-1}} = \frac{\Gamma_{n,n-1}}{\Gamma_{n-1,n}} \quad (63)$$

for $n = -s + 1, \dots, s - 1$. Together with the normalization requirement, this relation alone already determines the entire distribution $\{p_m\}$. In particular, it entails

$$\frac{p_{n+1}}{p_n} = \frac{\Gamma_{n+1,n}}{\Gamma_{n,n+1}}, \quad (64)$$

thus ensuring that also the second bracket in Eq. (62) vanishes, confirming detailed balance.

Now one needs to observe that the sign of the transition frequencies (60) depends on the relative magnitude of the driving frequency ω and the Rabi frequency Ω ; recall that the distinction between positive and negative transition frequencies — physically corresponding to the distinction between annihilation and creation of bath phonons — leads to the two different expressions (15) and (17) entering the transition rates (19). This prompts us to distinguish between the low-frequency case $0 < \omega < \Omega$ and the high-frequency case $0 < \Omega < \omega$ in the following. The resonant case $\omega = \Omega$ constitutes a special problem; this is best dealt with by taking the appropriate limits of the results obtained in the other two cases.

Finally, a further factor of substantial importance is the spectral density $J(\tilde{\omega})$, which may allow one to manipulate the quasistationary distribution to a considerable extent [42]. For the sake of simplicity and transparent discussion, here we assume that $J(\tilde{\omega}) \equiv J_0$ is constant.

A. Low-frequency case $0 < \omega < \Omega$

In order to utilize the above Eq. (64) for determining the distribution $\{p_m\}$ recursively we only need to evaluate the partial rates $\Gamma_{m,m+1}^{(\pm 1)}$ and $\Gamma_{m+1,m}^{(\pm 1)}$ according to the general prescription (19), making use of the particular representation (59). In the low-frequency case this leads to the expressions

$$\begin{aligned}\Gamma_{m,m+1}^{(\pm 1)} &= \frac{s(s+1) - m(m+1)}{16(1 - e^{-\beta(\Omega \mp \omega)})} \left(\frac{\Omega \mp \delta}{\Omega} \right)^2 \\ \Gamma_{m+1,m}^{(\pm 1)} &= \frac{s(s+1) - m(m+1)}{16(e^{\beta(\Omega \pm \omega)} - 1)} \left(\frac{\Omega \pm \delta}{\Omega} \right)^2\end{aligned}\quad (65)$$

which have been scaled by $\Gamma_0 = 2\pi\gamma^2 J_0$, and have thus been made dimensionless. Evidently, these representations imply that the desired ratio

$$\frac{\Gamma_{m+1,m}}{\Gamma_{m,m+1}} \equiv q_L \quad (66)$$

is independent of both s and m ; a tedious but straightforward calculation readily yields

$$q_L = \frac{2\delta\Omega \sinh(\beta\omega) + (\delta^2 + \Omega^2)(e^{-\beta\Omega} - \cosh(\beta\omega))}{2\delta\Omega \sinh(\beta\omega) - (\delta^2 + \Omega^2)(e^{\beta\Omega} - \cosh(\beta\omega))}. \quad (67)$$

Therefore, the quasistationary occupation probabilities of the Floquet states can be written in the form

$$p_m = \frac{1}{Z_L} q_L^m \quad (68)$$

with $m = -s, \dots, s$, and Z_L ensuring normalization. Hence, not only does one find detailed balance here, but the occupation probabilities even generate a finite geometric sequence.

B. High-frequency case $0 < \Omega < \omega$

Analogously, in the high-frequency case $0 < \Omega < \omega$ we require the dimensionless partial rates

$$\begin{aligned}\Gamma_{m,m+1}^{(\pm 1)} &= \pm \frac{s(s+1) - m(m+1)}{16(e^{\beta(\pm\omega - \Omega)} - 1)} \left(\frac{\Omega \mp \delta}{\Omega} \right)^2 \\ \Gamma_{m+1,m}^{(\pm 1)} &= \pm \frac{s(s+1) - m(m+1)}{16(e^{\beta(\Omega \pm \omega)} - 1)} \left(\frac{\Omega \pm \delta}{\Omega} \right)^2\end{aligned}\quad (69)$$

for constructing the matrix $\Gamma = \Gamma^{(1)} + \Gamma^{(-1)}$. Once more, the ratio

$$\frac{\Gamma_{m+1,m}}{\Gamma_{m,m+1}} \equiv q_H \quad (70)$$

does depend neither on s nor on m , so that the occupation probabilities again form a geometric sequence; after some juggling, one finds

$$q_H = \frac{(\delta^2 + \Omega^2) \sinh(\beta\omega) + 2\delta\Omega(e^{-\beta\Omega} - \cosh(\beta\omega))}{(\delta^2 + \Omega^2) \sinh(\beta\omega) - 2\delta\Omega(e^{\beta\Omega} - \cosh(\beta\omega))}. \quad (71)$$

Thus, the high-frequency Floquet-state occupation probabilities are given by

$$p_m = \frac{1}{Z_H} q_H^m \quad (72)$$

analogously to Eq. (68).

C. The quasitemperature

The fact that, on the one hand, the distribution of occupation probabilities $\{p_m\}$ is a geometric one in both the low- and the high frequency case, and that the quasienergy representatives ε_m of all Floquet states can be taken to be equidistant on the other, suggests to write this distribution in Boltzmann form,

$$p_m = \frac{1}{Z} \exp(-\vartheta \varepsilon_m), \quad (73)$$

where Z is adjusted such that this distribution is normalized, $\sum_{m=-s}^s p_m = 1$. Evidently, the parameter ϑ introduced here plays the role of an inverse *quasitemperature*, and Z is a formal analog of a canonical partition function [29]. We emphasize that we are dealing with a nonequilibrium steady state of the driven system which does not possess a temperature in the sense of equilibrium thermodynamics. However, this nonequilibrium steady state is characterized by a Boltzmannian distribution (73) into which a single parameter enters *as if* it were a temperature; hence, the designation “quasitemperature” is well justified. Needless to say, although the driven system is in contact with a bath which possesses a given temperature, its quasitemperature can be quite different from that temperature.

Evidently, the definition of such a quasitemperature still involves a certain degree of arbitrariness, as it requires to single out a specific representative of the quasienergy class of each Floquet state. In principle, one could employ the representatives

$$\varepsilon_m = m(\Omega + r\omega) \quad (74)$$

with arbitrary fixed $r \in \mathbb{Z}$ for integer s , and odd $r \in \mathbb{Z}$ for half-integer s ; this freedom can be exploited to equip the respective quasitemperature with properties deemed to

be desirable. For instance, when setting $r = +1$ ($r = -1$) for red (blue) detuning, one obtains representatives which for $F \rightarrow 0$ connect continuously to the energy eigenvalues of the undriven spin described by $H_0 = \omega_0 S_z$, thus guaranteeing that the quasitemperature introduced via these representatives reduces to the temperature of the ambient bath in the limit of vanishing driving amplitude.

Here we take a different route, and introduce a quasitemperature on the grounds of the representatives (53) and (54) selected earlier for computing the rates (19), so that the distribution acquires the practical form

$$p_m = \frac{1}{Z_q} \exp(-\vartheta \Omega m) \quad (75)$$

for both integer and half-integer s . Introducing, for ease of notation,

$$q \equiv \begin{cases} q_L & : 0 < \omega < \Omega \\ q_H & : 0 < \Omega < \omega \end{cases}, \quad (76)$$

with q_L and q_H as given by the expressions (67) and (71), respectively, this leads immediately to the definition

$$\vartheta \equiv -\frac{\ln q}{\Omega}. \quad (77)$$

Since q , being a ratio of two rates, may adopt any value between zero and $+\infty$, the quasitemperature then ranges from $-\infty$ to $+\infty$. Notwithstanding the various possible definitions of a quasitemperature, the very distribution $\{p_m\}$ itself, governing the observable physics, is determined uniquely. Also observe that, when $F \rightarrow 0$,

$$q \rightarrow \begin{cases} e^{-\beta \omega_0} & : \omega < \omega_0 \\ e^{+\beta \omega_0} & : \omega > \omega_0 \end{cases}. \quad (78)$$

Hence, in the absence of the time-periodic driving field the above solutions (68) and (72) correctly lead to a Boltzmann distribution with the inverse bath temperature β , thereby indicating thermal equilibrium of the spin system; the unfamiliar “plus”-sign appearing in this limit (78) in the case of blue detuning merely reflects the reversed labeling already discussed in the paragraph following Eq. (54).

The dimensionless inverse quasitemperature $\omega_0 \vartheta$ ultimately depends on the scaled driving amplitude F/ω_0 , the scaled driving frequency ω/ω_0 , and the dimensionless inverse actual temperature $\omega_0 \beta$ of the heat bath, but not on the spin quantum number s . In contrast, the partition function Z_q depends on s :

$$Z_q = \sum_{m=-s}^s \exp(-\vartheta \Omega m) = \frac{\sinh\left(\frac{2s+1}{2} \vartheta \Omega\right)}{\sinh\left(\frac{\vartheta \Omega}{2}\right)}. \quad (79)$$

The inverse quasitemperature ϑ vanishes — meaning that the periodically driven system effectively becomes infinitely hot, so that all its Floquet states are populated

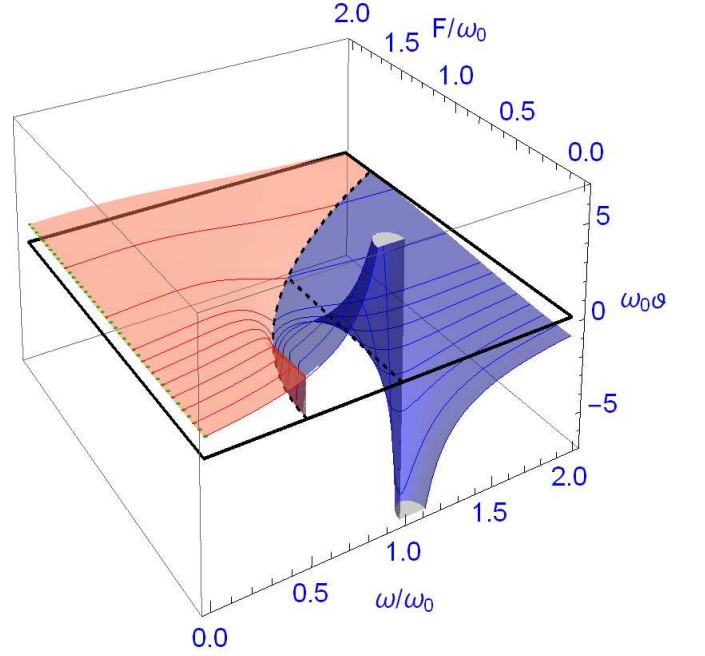


FIG. 1: (Color online) Dimensionless inverse quasitemperature $\omega_0 \vartheta$ of the spin system under the influence of a circularly polarized monochromatic driving force with amplitude F and frequency ω , being coupled to a harmonic-oscillator bath of inverse actual temperature $\omega_0 \beta = 1$. The blue (dark) part of the graph corresponds to the high-frequency regime $0 < \Omega < \omega$, the red (gray) part to the low-frequency regime $0 < \omega < \Omega$. Along the line segment $\omega = \omega_0$ with $F < \omega_0$ and along the parabola $\omega = \omega_c$ given by Eq. (80), both marked by black dashes, the inverse quasitemperature vanishes. A few functions $\vartheta(\omega)$ for constant F are highlighted. The limit $\omega_0 \vartheta = \omega_0 \beta$ for $\omega/\omega_0 \rightarrow 0$ is indicated by a green (dotted) line.

equally — regardless of the bath temperature, if either $\omega = \omega_0$ while $0 < F < \omega_0$, or if

$$\omega = \omega_c \equiv \frac{1}{2\omega_0} (F^2 + \omega_0^2), \quad (80)$$

with the latter equation defining the boundary $\omega = \Omega$ between the low- and the high-frequency regime, see Figs. 1 and 2. Along this boundary the quasienergies of all Floquet states are degenerate (modulo ω), so that the appearance of infinite quasitemperature here can be understood as a resonance effect. In terms of the inverse quasitemperatures, denoted ϑ_L (ϑ_H) in the low- (high-) frequency regime, there is a continuous change from ϑ_L to ϑ_H , since

$$\lim_{\omega \uparrow \omega_c} \vartheta_L = \lim_{\omega \downarrow \omega_c} \vartheta_H = 0. \quad (81)$$

However, the two functions ϑ_L and ϑ_H do not join smoothly at $\omega = \omega_c$, since their derivatives with respect

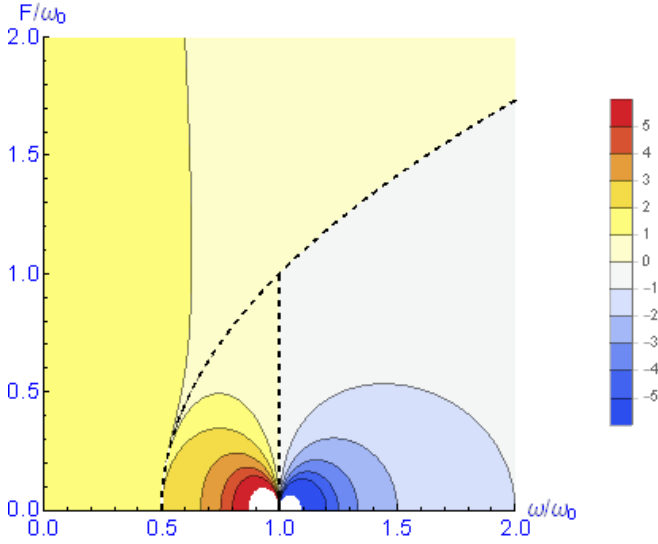


FIG. 2: (Color online) Contour plot of the dimensionless inverse quasitemperature $\omega_0\vartheta$ with the same parameters as in Figure 1. The line segment $\omega = \omega_0$ with $F < \omega_0$ and the parabola $\omega = \omega_c$, where ϑ vanishes, are again marked by black dashes.

to ω adopt different limits:

$$\begin{aligned} \lim_{\omega \uparrow \omega_c} \frac{\partial \vartheta_L}{\partial \omega} &= -\frac{4\beta\omega_0^3 (F^4 + \omega_0^4)}{F^4 (F^2 + \omega_0^2)^2}, \\ \lim_{\omega \downarrow \omega_c} \frac{\partial \vartheta_H}{\partial \omega} &= \frac{4\beta\omega_0^3 (F - \omega_0) (F + \omega_0)}{F^4 (F^2 + \omega_0^2)}. \end{aligned} \quad (82)$$

We will now investigate the behavior of the function $\omega_0\vartheta(\omega_0\beta, \omega/\omega_0, F/\omega_0)$ in the limits corresponding to the four sideways faces of the box bounding the plot displayed in Fig. 1:

(i) As already noted at the end of Sec. III B, in the low-frequency limit $\omega/\omega_0 \rightarrow 0$ the quasienergies (53) and (54) approach the actual energies $E_m = m\sqrt{\omega_0^2 + F^2}$ (with $m = s, \dots, -s$) of a spin exposed to a slowly varying drive. Hence, in this limit the periodic thermodynamics investigated here must reduce to the usual thermodynamics described by a canonical ensemble; in particular, the inverse quasitemperature ϑ must approach the true inverse bath temperature β . This expectation is borne out by the leading term of the low-frequency expansion

$$\begin{aligned} \omega_0\vartheta_L &= \omega_0\beta + \frac{2\omega_0\beta(\omega/\omega_0)}{(F/\omega_0)^2 + 2} \\ &+ \frac{\omega_0\beta(\omega/\omega_0)^2}{2((F/\omega_0)^2 + 2)^2} \left(8 - 4(F/\omega_0)^2 - \frac{(F/\omega_0)^4 \omega_0\beta \coth\left(\frac{\omega_0\beta}{2}\sqrt{(F/\omega_0)^2 + 1}\right)}{\sqrt{(F/\omega_0)^2 + 1}} \right) + O(\omega/\omega_0)^3. \end{aligned} \quad (83)$$

(ii) Next we consider the ultrahigh-frequency limit $\omega/\omega_0 \rightarrow \infty$, keeping both $\omega_0\beta$ and F/ω_0 fixed. Inspecting q_H as defined by Eq. (71), and observing that asymptotically $\Omega = \sqrt{(\omega_0 - \omega)^2 + F^2} \sim \omega - \omega_0$ for $\omega/\omega_0 \rightarrow \infty$, one finds $q_H \rightarrow \exp(+\beta\omega_0)$. Recalling the reversed labeling of Floquet states for blue detuning, which accounts for the “plus” sign, this implies that in this limit the Floquet-state distribution (72) equals the Boltzmann distribution for the undriven energy eigenstates with the bath temperature. This finding can intuitively be understood as an averaging principle: In the ultrahigh-frequency limit the effect of the external drive on the occupation probabilities averages out, leaving one with the original thermal distribution. On the other hand, there is no such averaging principle for quasienergies; the ac Stark shift (that is, the deviation of the quasienergies from the energy eigenvalues of the undriven system) increases as ω . Since our quasitemperature is defined with respect to the quasienergies, it follows that the quasitemperature has to vanish at high frequencies: By virtue of Eq. (77) one has

$\vartheta_H \sim -\beta\omega_0/\omega$, and hence

$$\lim_{\omega/\omega_0 \rightarrow \infty} \omega_0\vartheta_H = 0; \quad (84)$$

as shown by Fig. 1, this limit is approached with negative quasitemperatures.

(iii) The static limit of vanishing driving amplitude, $F/\omega_0 \rightarrow 0$, yields

$$\lim_{F/\omega_0 \rightarrow 0} \omega_0\vartheta_L = \lim_{F/\omega_0 \rightarrow 0} \omega_0\vartheta_H = \frac{\omega_0\beta}{1 - \omega/\omega_0}, \quad (85)$$

easily deduced from the limits (78) in combination with the definition (77). Once again, this seemingly strange expression, exhibiting a pole at $\omega = \omega_0$ which is prominently visible in Fig. 1, is fully in agreement with the requirement that the periodic thermodynamics should reduce to ordinary thermodynamics when the time-periodic driving force vanishes. Namely, for $F/\omega_0 \rightarrow 0$ the system possesses the energy eigenvalues $E_m = m\omega_0$, whereas the quasienergy representatives (53) or (54) reduce to $\varepsilon_m = m|\omega_0 - \omega|$ or $\varepsilon_m = \omega/2 + m|\omega_0 - \omega|$ with $m = s, \dots, -s$, while the Floquet states approach

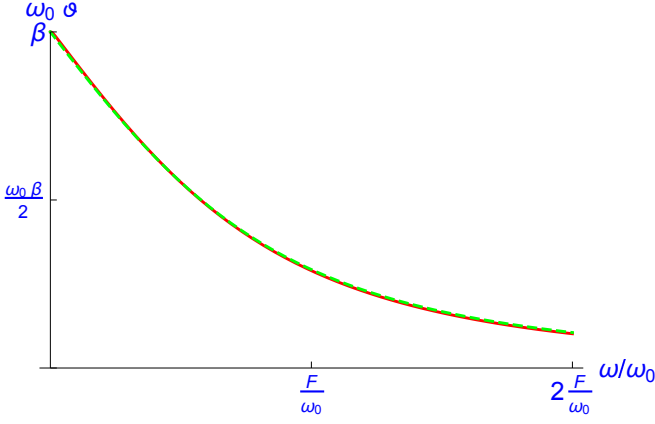


FIG. 3: (Color online) Inverse dimensionless quasitemperature $\omega_0\vartheta$ for $\omega_0\beta = 1$ and $F/\omega_0 = 100$ as a function of ω/ω_0 in the regime $0 < \omega/\omega_0 < 2F/\omega_0$. We show the exact values of $\omega_0\vartheta_L$ (red line), as well as the asymptotic form (86) (green dashes).

the energy eigenstates of $H_0 = \omega_0 S_z$. In this limit the parametrization of their occupation probabilities in terms of either the quasithermal distribution (73) or the standard canonical distribution must lead to identical values, implying that the usual Boltzmann factor $\exp(-\beta m \omega_0)$ must become proportional to $\exp(-\vartheta m |\omega_0 - \omega|)$. Hence, one has $\beta \omega_0 = \vartheta(\omega_0 - \omega)$ for $F/\omega_0 \rightarrow 0$ and $0 < \omega < \omega_0$, which immediately furnishes the above expression (85). In the case of blue detuning, for $0 < \omega_0 < \omega$, the reversed labeling of the quasienergies yields an additional “minus” sign, again leading to the limit (85).

(iv) In the converse strong-driving limit $F/\omega_0 \rightarrow \infty$ we first focus on the regime $\omega \sim F$ where $\vartheta = \vartheta_L > 0$. After some transformations we obtain the asymptotic form

$$\omega_0\vartheta_L \sim \omega_0\beta - \frac{\omega\beta}{\sqrt{(F/\omega_0)^2 + (\omega/\omega_0)^2}} \quad (86)$$

in this regime, so that the inverse quasitemperature decreases monotonically with increasing driving amplitude, as exemplified by Fig. 3.

In contrast, for $\omega > \omega_c$ as given by Eq. (80) we have $\vartheta = \vartheta_H < 0$. Asymptotically, here we find

$$\omega_0\vartheta_H \sim -\frac{\omega_0\beta}{\omega/\omega_0} + \frac{\omega_0\beta}{2(\omega/\omega_0)^2} (F/\omega_0)^2. \quad (87)$$

This asymptotic function exhibits a pronounced minimum at $\omega/\omega_0 = (F/\omega_0)^2$ of depth $\omega_0\vartheta_H \sim -\omega_0^3\beta/(2F^2)$, depicted in Fig. 4. This minimum can be understood as a result of two opposing trends: On the one hand, the averaging principle requires that the occupation probabilities approach the “undriven” Boltzmann distribution with the bath temperature for large ω/ω_0 , which means that the inverse quasitemperature tends to a finite value proportional to $-\beta$ for large, but finite driving frequencies. On the other hand, the factor $1/\Omega$ in Eq. (77) becomes more and more predominant and forces ϑ to approach 0 in the high-frequency regime.

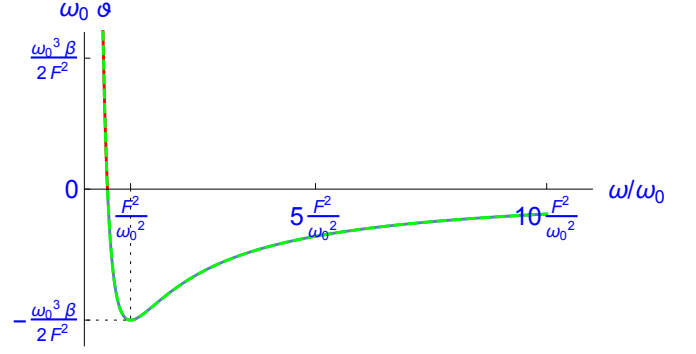


FIG. 4: (Color online) Inverse dimensionless quasitemperature $\omega_0\vartheta$ for $\omega_0\beta = 1$ and $F/\omega_0 = 100$ as a function of ω/ω_0 in the regime $\omega/\omega_0 > (F/\omega_0)^2/2$. We show the exact values of $\omega_0\vartheta_L$ (red solid line) and $\omega_0\vartheta_H$ (blue solid line), together with the asymptotic form (87) (green dashes).

V. APPLICATION: PERIODICALLY DRIVEN PARAMAGNETS

A. Calculation of quasithermal expectation values

Starting from the proposition that the Floquet states of a periodically driven spin system be populated according to the distribution (73) we introduce the quasithermal average of the spin component in the direction of the static field,

$$\langle S_z \rangle_q \equiv \frac{1}{Z} \sum_{m=-s}^s \langle u_m(t) | S_z | u_m(t) \rangle \exp(-\vartheta \varepsilon_m). \quad (88)$$

In order to evaluate this expression we utilize the representation (52) of the Floquet functions, giving

$$\begin{aligned} Z \langle S_z \rangle_q &= \sum_{m=-s}^s \langle m | P^{(s)\dagger} S_z P^{(s)} | m \rangle \exp(-\vartheta \varepsilon_m) \\ &= \text{Tr} \left(P^{(s)\dagger} S_z P^{(s)} \exp(-\vartheta G^{(s)}) \right). \end{aligned} \quad (89)$$

Next, we resort once more to the lifting technique: For $s = 1/2$, the decomposition (42) readily yields

$$\begin{aligned} P^\dagger s_z P &= \Xi^\dagger s_z \Xi \\ &= \frac{\delta}{\Omega} s_z - \frac{\sqrt{\Omega^2 - \delta^2}}{\Omega} s_x \end{aligned} \quad (90)$$

by virtue of Eq. (45). Applying the irrep $r^{(s)}$, we deduce

$$\begin{aligned} P^{(s)\dagger} S_z P^{(s)} &= r^{(s)}(P^\dagger s_z P) \\ &= \frac{\delta}{\Omega} S_z - \frac{\sqrt{\Omega^2 - \delta^2}}{\Omega} S_x. \end{aligned} \quad (91)$$

Inserting this into the above identity (89), and calculating the trace in the eigenbasis of S_z , we obtain the important result

$$\langle S_z \rangle_q = \frac{1}{Z_q} \frac{\omega_0 - \omega}{\Omega} \sum_{m=-s}^s m e^{-\vartheta \Omega m}, \quad (92)$$

valid for both integer and half-integer s . In particular, this shows that the quasithermal expectation value (88) does not depend on time, despite the time-dependence of the Floquet functions. Although the unusual-looking prefactor $(\omega_0 - \omega)/\Omega$ indeed implies that the z -component of the magnetization vanishes for $\omega = \omega_0$, it does not necessarily imply that the magnetization reverses its direction when ω is varied across ω_0 , since the reversal of the prefactor's sign can be compensated by a simultaneous change of the sign of the quasitemperature, as it happens for low driving amplitudes according to Eq. (85).

B. Response of paramagnetic materials to circularly polarized driving fields

As an experimentally accessible example of the above considerations, and thus as a possible laboratory application of periodic thermodynamics, we consider the magnetization of an ideal paramagnetic substance under the influence of both a static magnetic field applied in the z -direction, and a circularly polarized oscillating magnetic field applied in the x - y -plane. In order to facilitate comparison with the literature, here we re-install the Planck constant \hbar and the Boltzmann constant k_B .

We assume that the magnetic atoms of the substance have an electron shell with total angular momentum J , resulting from the coupling of orbital angular momentum and spin, giving the magnetic moment $\mu = g_J \mu_B J$. Here μ_B denotes the Bohr magneton, and g_J is the Landé g -factor which may assume both signs; for the sake of definiteness, here we assume $g_J < 0$. In the presence of a constant magnetic field B_0 this moment gives rise to the energy levels

$$E_m = -m g_J \mu_B B_0 \equiv m \hbar \omega_0, \quad (93)$$

where $m = -J \dots, J$ is the magnetic quantum number. Hence, with $g_J < 0$ the spin tends to align antiparallel to the applied magnetic field, favoring $m = -J$.

Let us briefly recall the usual textbook treatment of the ensuing thermal paramagnetism within the canonical ensemble [28, 29], assuming the substance to possess a temperature T . Then the canonical partition function

$$\begin{aligned} Z_0 &= \sum_{m=-J}^J \exp\left(-\frac{E_m}{k_B T}\right) = \sum_{m=-J}^J \exp\left(-m \frac{\hbar \omega_0}{k_B T}\right) \\ &= \frac{\sinh\left(\frac{2J+1}{2J} y_0\right)}{\sinh\left(\frac{y_0}{2J}\right)} \end{aligned} \quad (94)$$

which depends on the dimensionless quantity

$$y_0 \equiv -\frac{g_J \mu_B B_0}{k_B T} J = \frac{\hbar \omega_0}{k_B T} J \quad (95)$$

serves as moment-generating function, in the sense that the thermal expectation value of the magnetization M

is obtained by taking the appropriate derivative of its logarithm, namely,

$$\begin{aligned} \langle M \rangle &= \frac{N}{V} \langle \mu \rangle = \frac{N}{V} g_J \mu_B \langle m \rangle \\ &= \frac{N}{V} \frac{\partial}{\partial B_0} k_B T \ln Z_0. \end{aligned} \quad (96)$$

Here N/V denotes the density of contributing atoms. Working out this prescription, one finds the magnetization [28, 29]

$$\langle M \rangle = M_0 B_J(y_0), \quad (97)$$

where

$$M_0 = -\frac{N}{V} g_J \mu_B J \quad (98)$$

denotes the saturation magnetization, and

$$B_J(y) \equiv \frac{2J+1}{2J} \coth\left(\frac{2J+1}{2J} y\right) - \frac{1}{2J} \coth\left(\frac{y}{2J}\right) \quad (99)$$

is the so-called Brillouin function of order J [26]; this theoretical prediction (97) has been beautifully confirmed in low-temperature experiments with paramagnetic ions by Henry [27] already in 1952. In the weak-field limit $\mu_B B_0 \ll k_B T$ one may use to approximation

$$B_J(y) \approx \frac{J+1}{J} \frac{y}{3} \quad \text{for } |y| \ll 1, \quad (100)$$

giving

$$\langle M \rangle \approx \frac{N}{V} \frac{(g_J \mu_B)^2 J(J+1)}{3 k_B T} B_0. \quad (101)$$

Returning to periodic thermodynamics, let us add the circularly polarized field $B_1(\cos \omega t, \sin \omega t, 0)$ perpendicularly to the constant one. Then the Rabi frequency (38) can be written as

$$\Omega = \sqrt{(\omega_0 - \omega)^2 + (g_J \mu_B B_1 / \hbar)^2}, \quad (102)$$

where

$$\omega_0 = -\frac{g_J \mu_B B_0}{\hbar} \quad (103)$$

measures the strength of the static field in accordance with Eq. (93). Assuming that the spins' environment is correctly described by a thermal oscillator bath with constant spectral density J_0 , and the coupling to that environment is given by the expression (55), the Floquet-state occupation probabilities are governed by the distribution (73), and we can invoke the above result (92) to write the observable magnetization in the form

$$\begin{aligned} \langle M \rangle_q &= -\frac{N}{V} g_J \mu_B \langle S_z \rangle_q \\ &= -\frac{N}{V} \frac{g_J \mu_B}{Z_q} \frac{\omega_0 - \omega}{\Omega} \sum_{m=-J}^J m \exp\left(-m \frac{\hbar \Omega}{k_B T}\right), \end{aligned} \quad (104)$$

where $\tau = 1/(k_B\vartheta)$ is the quasitemperature, and

$$Z_q = \sum_{m=-J}^J \exp\left(-m \frac{\hbar\Omega}{k_B\tau}\right) \quad (105)$$

is the corresponding partition function (79). Quite remarkably, this expression (104) is a perfect formal analog of the previous Eq. (96), since we have

$$\langle M \rangle_q = \frac{N}{V} \frac{\partial}{\partial B_0} k_B\tau \ln Z_q, \quad (106)$$

taking into account the nonlinear dependence of the Rabi frequency (102) on the static field strength B_0 . Hence, the resulting quasithermal magnetization can be expressed in a manner analogous to Eq. (97), namely,

$$\langle M \rangle_q = M_1 B_J(y_1), \quad (107)$$

with modified saturation magnetization

$$M_1 = \frac{\omega_0 - \omega}{\Omega} M_0, \quad (108)$$

and the argument of the Brillouin function now depending on the quasitemperature,

$$y_1 = \frac{\hbar\Omega}{k_B\tau} J. \quad (109)$$

For consistency, this prediction (107) must reduce to the usual weak-field magnetization (101) when both $B_1 \rightarrow 0$ and $\mu_B B_0 \ll k_B T$. This is ensured by the limit (85): For sufficiently small B_1 , the quasitemperature τ is related to the actual bath temperature T through

$$\frac{1}{k_B\tau} \approx \frac{\omega_0}{\omega_0 - \omega} \frac{1}{k_B T}. \quad (110)$$

Inserting this into Eq. (107), one can employ the approximation (100) for frequencies ω not too close to ω_0 . In this way one recovers the expected expression (101) unless $\omega \approx \omega_0$, in which case one has $\langle M \rangle_q \approx 0$.

As is evident from the above discussion, under typical conditions of electron spin resonance (ESR) with weak driving amplitudes, such that B_1/B_0 is on the order of 10^{-2} or less [43], the difference between the quasithermal magnetization $\langle M \rangle_q$ and the customary thermal magnetization $\langle M \rangle$ is more or less negligible, except for driving frequencies close to resonance. This is illustrated in Fig. 5 for $g_J \mu_B B_1/(\hbar\omega) = 0.01$, where the bath temperature is chosen such that $k_B T = \hbar\omega$. Here we have plotted both the usual magnetization (97) of an undriven spin system and the quasithermal magnetization (107) of its weakly driven counterpart, normalized to their respective saturation value, vs. the ratio ω_0/ω , representing the scaled strength B_0 of the static field. The vanishing of the quasithermal magnetization at both $\omega_0/\omega = 1$ and $\omega_0/\omega = 2$ clearly reflects the appearance of infinite quasitemperature at these ratios, as already observed in Fig. 1.

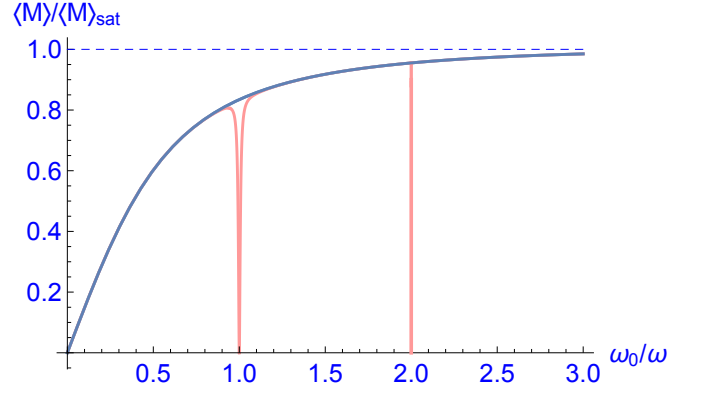


FIG. 5: (Color online) Magnetizations $\langle M \rangle$ divided by their saturation magnetizations as functions of the scaled strength ω_0/ω of the static field. The blue (dark) curve represents the ordinary thermal magnetization (97), the red (gray) one the quasithermal magnetization (107) for weak driving, $g_J \mu_B B_1/(\hbar\omega) = 0.01$. Here we have set $k_B T = \hbar\omega$ and $J = 7/2$.

In marked contrast, novel types of behavior with measurable consequences occur in the regime of non-perturbatively strong driving. A particularly striking example is provided by Fig. 6, where $k_B T = \hbar\omega_0$ and $J = 1$: Under strong driving, the ratio $\langle M \rangle_q / \langle M \rangle$ actually becomes *negative* for frequencies $\omega_0 < \omega < \omega_c$, implying that the paramagnetic material effectively becomes a diamagnetic one, reflecting the fact that under strong driving the distribution of Floquet-state occupation probabilities can differ substantially from the original thermal Boltzmann distribution. This possibility of turning a paramagnet into a diamagnet through the application of strong time-periodic forcing, as further elucidated in Fig. 7, is a “hard” prediction of periodic thermodynamics which now awaits its experimental verification.

VI. DISSIPATION

Since a bath-induced transition from a Floquet state n to a Floquet state m is accompanied by all frequencies $\omega_{mn}^{(\ell)}$ as introduced in Eq. (9), the rate of energy dissipated in the quasistationary state is given by [30]

$$R = - \sum_{mn\ell} \omega_{mn}^{(\ell)} \Gamma_{mn}^{(\ell)} p_n. \quad (111)$$

For consistency it needs to be shown that $R > 0$, so that in the nonequilibrium steady state characterized by the Floquet-state distribution $\{p_n\}$ the energy flows from the driven system into the bath, regardless of the system’s quasitemperature [42]. While this intuitive expression yields the mean dissipation rate, it is, in principle, also possible to obtain the full probability distribution of energy exchanges between a periodically driven quantum system and a thermalized heat reservoir by applying the methods developed in Ref. [44].

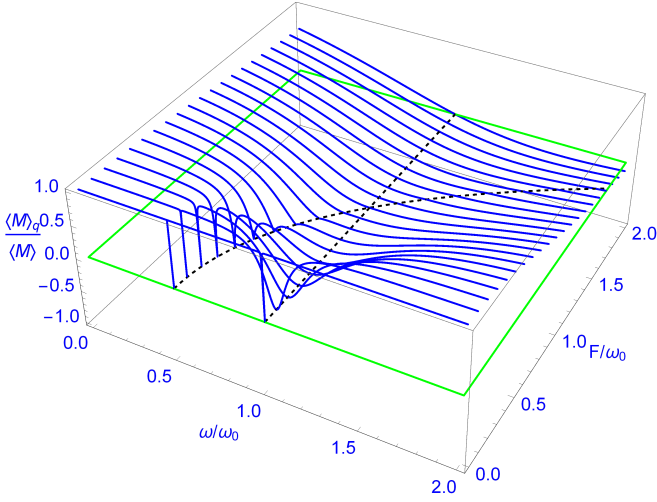


FIG. 6: (Color online) Ratio $\langle M \rangle_q / \langle M \rangle$ of the quasithermal magnetization (107) and the customary magnetization (97) as function of ω/ω_0 and F/ω_0 , with $F = g_J \mu_B B_1 / \hbar$. Parameters chosen here are $k_B T = \hbar \omega_0$ and $J = 1$. Along the dashed black line $\omega = \omega_0$ and along the dashed black parabola $\omega = \omega_c$ given by Eq. (80) the quasithermal magnetization vanishes, so that $\langle M \rangle_q / \langle M \rangle$ becomes negative for strong driving with frequencies $\omega_0 < \omega < \omega_c$.

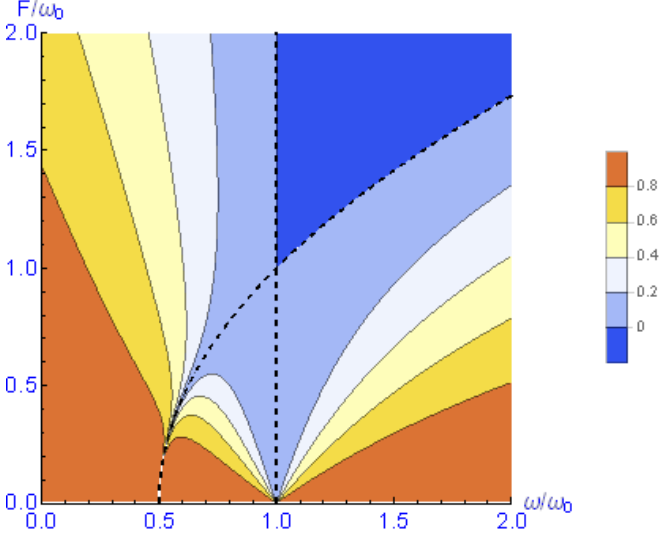


FIG. 7: (Color online) Contour plot of the ratio $\langle M \rangle_q / \langle M \rangle$ with the same parameters as in Fig. 6. The domain in which $\langle M \rangle_q / \langle M \rangle$ becomes negative is indicated by the dark blue color.

The expression (111) can now be evaluated for all spin quantum numbers s . In addition to the partial transition rates (19) for neighboring Floquet states $m = n \pm 1$ listed in Secs. IV A and IV B, Eq. (111) also requires the rates for pseudotransitions with $m = n$. Again dividing by $\Gamma_0 = 2\pi\gamma^2 J_0$, we obtain the dimensionless diagonal

transition rates

$$\Gamma_{mm}^{(\pm 1)} = \pm \frac{(2m)^2 F^2}{16 (e^{\pm \beta \omega} - 1) \Omega^2} \quad (112)$$

for $m = s, \dots, -s$, valid for both cases $0 < \omega < \Omega$ and $0 < \Omega < \omega$. In order to represent R in a condensed fashion we define the polynomials

$$\begin{aligned} P_s(q) &\equiv -2 \sum_{m=0}^{2s} (m-s)^2 q^m \\ Q_s(q) &\equiv \frac{1}{2} \sum_{m=0}^{2s-1} (m+1)(2s-m) q^m \\ z_s(q) &\equiv \sum_{m=0}^{2s} q^m, \end{aligned} \quad (113)$$

together with the expression

$$A^\pm(q) \equiv \frac{(e^{\beta(\pm\omega+\Omega)} q - 1) (\delta \pm \Omega)^2 (\omega \pm \Omega)}{e^{\beta(\pm\omega+\Omega)} - 1}. \quad (114)$$

Dividing by $\omega_0 \Gamma_0$, one obtains a dimensionless dissipation rate which can now be written in the form

$$R = \frac{P_s(q) \omega F^2 + Q_s(q) (A^+(q) \mp A^-(q))}{8 z_s(q) \Omega^2}, \quad (115)$$

where one has to insert either q_L or q_H for q , in accordance with the case distinction (76), and the “ \mp ”-sign in the numerator becomes “minus” for $0 < \omega < \Omega$, but “plus” for $0 < \Omega < \omega$.

After resolving all symbols R will be a function of five arguments, $R = R(s, \beta, \omega, \omega_0, F)$, which makes the discussion more difficult than in the case of $s = 1/2$ that has been considered in Ref. [30]. Thus, here we mention only the most perspicuous aspects of the dissipation function.

Recall that for both $\omega = \omega_0$ with $0 < F < \omega_0$ and $\omega = \omega_c = (F^2 + \omega_0^2)/(2\omega_0)$ we have $q = 1$, and hence $\vartheta = 0$. It turns out that along these two curves in the (ω, F) -plane the dimensionless rate R takes on the value

$$R_0 = \frac{1}{6} s(s+1), \quad (116)$$

as visualized in Figs. 8 and 9 for $s = 1$ and $s = 10$, respectively. For $1/2 \leq s \leq 7/2$ this value constitutes a smooth maximum for $\omega = \omega_0$ and small F/ω_0 which becomes increasingly sharp for $F/\omega_0 \rightarrow 0$. However, for $s > 7/2$ the previous maximum turns into a local minimum, the sharpness of which increases for $s \rightarrow \infty$. In contrast, along the line $\omega = \omega_c$ this value R_0 remains a local maximum of R for all s , as long as $F < \omega_0$.

For $s \rightarrow \infty$ the scaled dissipation rate $r \equiv R/(s^2 + s)$ tends to the limit

$$r_\infty(\omega/\omega_0, F/\omega_0) \equiv \frac{\omega}{4\omega_0} \frac{F^2}{F^2 + (\omega - \omega_0)^2} \quad (117)$$

which is independent of the heat-bath temperature. As illustrated by Fig. 10 the convergence proceeds pointwise

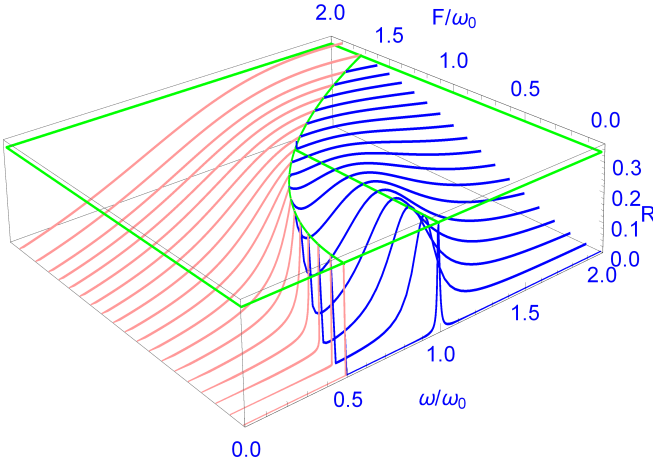


FIG. 8: (Color online) The dimensionless dissipation rate R for $s = 1$ and $\omega_0\beta = 1$ as a function of ω/ω_0 and F/ω_0 . The blue (dark) part of the graph corresponds to the high-frequency regime $0 < \Omega < \omega$, the red (gray) one to the low-frequency regime $0 < \omega < \Omega$. Along the line $\omega = \omega_0$ with $0 < F < \omega_0$ and along the parabola $\omega = \omega_c$ given by Eq. (80) the dissipation rate takes on the constant value $s(s+1)/6 = 1/3$ (green solid lines and parabola).

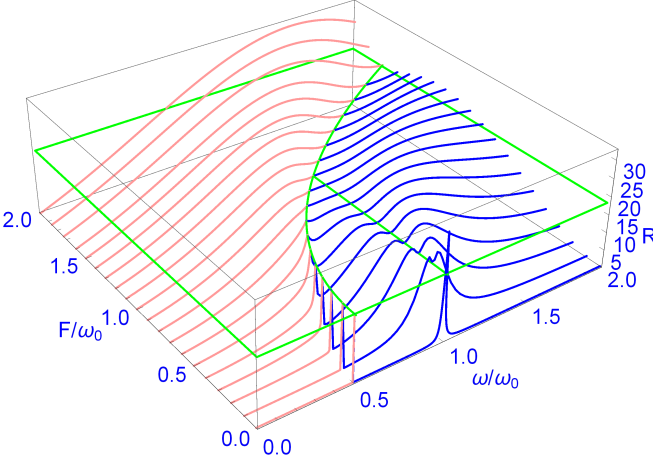


FIG. 9: (Color online) As Fig. 8, but for $s = 10$. Along the line $\omega = \omega_0$ with $0 < F < \omega_0$ and along the parabola $\omega = \omega_c$ given by Eq. (80) the dissipation rate takes on the constant value $s(s+1)/6 = 55/3$ (green solid lines and parabola). The blue (dark) curve with $F/\omega_0 \approx 0$ possesses two unresolved sharp maxima close to an equally sharp minimum at $\omega \approx \omega_0$.

except for $\omega = \omega_c$ and $\omega = \omega_0$ when $F < \omega_0$, where $r = 1/6$ for all s . For fixed F the asymptotic function $r_\infty(\omega/\omega_0, F/\omega_0)$ has a global maximum at

$$\omega_m/\omega_0 = \sqrt{(F/\omega_0)^2 + 1}, \quad (118)$$

adopting the value

$$r_m = \frac{1}{8} \left(1 + \sqrt{(F/\omega_0)^2 + 1} \right), \quad (119)$$

as depicted in Figs. 10 and 11. Interestingly, the shape

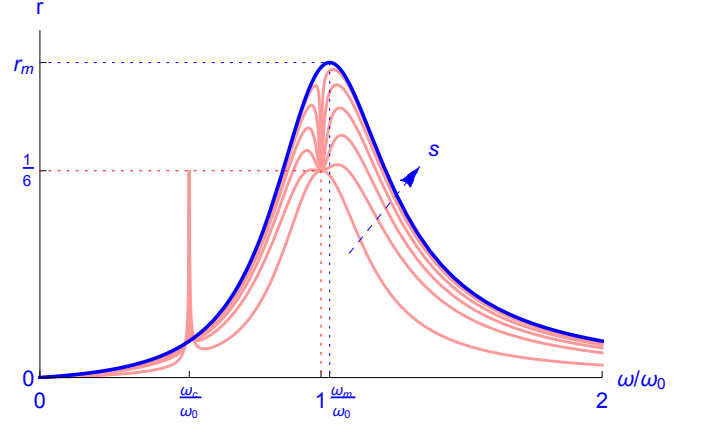


FIG. 10: (Color online) The scaled dissipation rate $r = R/(s^2 + s)$ for $s = 1/2, 5, 10, 20, 50, 200$, with bath temperature $\omega_0\beta = 1$ and driving amplitude $F/\omega_0 = 1/4$, as a function of ω/ω_0 . The six red (gray) curves increase with s for $\omega > \omega_c$ as indicated by the dashed arrow. They all meet at the two points with coordinates $(\omega_c/\omega_0, 1/6)$ and $(1, 1/6)$. The asymptotic envelope (117) is given by the blue (dark) curve, with its maximum $(\omega_m/\omega_0, r_m)$ being determined by Eqs. (118) and (119).

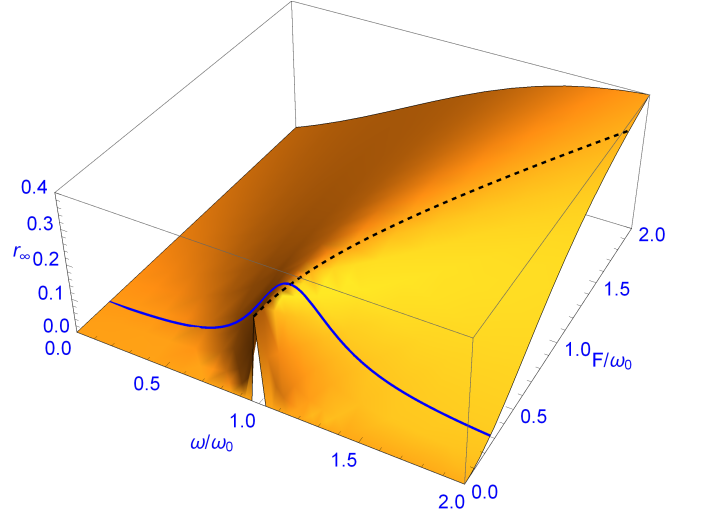


FIG. 11: (Color online) The asymptotic limit $r_\infty(\omega/\omega_0, F/\omega_0)$ of the scaled dissipation rate $R/(s^2 + s)$ for $s \rightarrow \infty$ according to Eq. (117). The particular curve with $F/\omega_0 = 1/4$ considered in Fig. 10 is shown in blue color (dark solid curve). The maximum values of the functions $r_\infty(\omega/\omega_0, F/\omega_0)$ with constant F according to Eqs. (118) and (119) are indicated by a black dashed curve.

of r_∞ as a function of ω/ω_0 , indicating a resonance phenomenon leading to a maximum of the absorbed heat at $\omega = \omega_m$ close to ω_0 , is closely related to a prediction based on the classical Landau-Lifshitz equation [?], as sketched briefly in Appendix B.

VII. DISCUSSION

A simple harmonic oscillator which is linearly driven by an external time-periodic force while kept in contact with a thermal oscillator bath represents a nonequilibrium system, but nonetheless adopts a steady state and develops a quasistationary distribution of Floquet-state occupation probabilities which equals the Boltzmann distribution of the equilibrium model obtained in the absence of the driving force, being characterized by precisely the same temperature as that of the bath it is coupled to [11, 30].

The system considered in the present work, a spin with arbitrary spin quantum number s exposed to a circularly polarized driving field while interacting with a bath of thermally occupied harmonic oscillators, may be regarded as the next basic model in a hierarchy of analytically solvable models on Periodic Thermodynamics. Exactly as in the case of the linearly forced harmonic oscillator, the system-bath interaction here induces nearest-neighbor coupling among the Floquet states of the time-periodically driven system, so that the model's transition matrix (18) is tridiagonal, thus enforcing detailed balance. Again, the resulting quasistationary Floquet distribution turns out to be Boltzmannian, but now with a quasitemperature which differs from the physical temperature of the bath. Already the mere fact that a time-periodically driven quantum system in its steady state may exhibit a quasitemperature which is different from the actual temperature of its environment, and which can be actively controlled by adjusting, *e.g.*, the amplitude or frequency of the driving force, in itself constitutes a noteworthy observation, suggesting that periodic thermodynamics generally may be far more subtle than usual equilibrium thermodynamics based on some effective Floquet Hamiltonian.

For systems exhibiting a geometric distribution $\{p_n\}$ of Floquet-state occupation probabilities, the parametrization of the latter in terms of a quasitemperature is feasible if there are equidistant canonical representatives of the respective quasienergy classes [42]. Therefore, we conjecture that the possibility to introduce a quasitemperature remains restricted to particularly simple integrable systems. However, the concept of quasistationary Floquet-state occupation probabilities does not require the introduction of a quasitemperature, and the exploration of the dependence of the corresponding observable quasistationary expectation values on the parameters of the driven system and its coupling to its environment constitutes a major task of periodic thermodynamics in general.

In this sense our model system is not only of basic theoretical interest, but also leads to novel predictions concerning future experiments with paramagnetic materials in strong circularly polarized fields. The very existence of a quasistationary Floquet distribution which is different from the distribution characterizing thermal equilibrium implies that the magnetic response of such a periodically driven material can be quite different from that of the un-

driven one; as we have demonstrated in Sec. V B, a strong circularly polarized driving field effectively may turn a paramagnetic material into a diamagnetic one. While we are not in a position to ascertain whether the corresponding parameter regime can be reached with already existing experimental set-ups [46], it might be worthwhile to design specifically targeted measurements for confirming this particularly striking prediction of periodic thermodynamics.

Yet, there is still more at stake here. When Brillouin published his now-famous treatise [26] on thermal paramagnetism in 1927, this was essentially a blueprint for an experimental demonstration of the quantization of angular momentum, whereas the further thermodynamical input into the theory was not to be questioned, being backed by the overwhelming generality of equilibrium thermodynamics [28, 29]. At the advent of periodic thermodynamics more than 90 years later, one faces an inverted situation: With the quantization of angular momentum being firmly established, it is nonequilibrium physics in the guise of periodic thermodynamics which is to be examined in measurements of paramagnetism under time-periodic driving. As has been stressed already by Kohn [10] and clarified by Breuer *et al.* [11], quasistationary Floquet distributions are not universal, depending on the very form of the system-bath interaction. Here we have assumed an interaction of the simplistic type (11) with coupling (55) proportional to the spin operator S_x on the system's side and simple creation and annihilation operators (13) on the side of the bath, combined with the assumption of a constant spectral density of the bath, but there are other possibilities. Measurements of magnetism under strong driving will be sensitive to such issues; two materials which exhibit precisely the same paramagnetic response in the absence of time-periodic forcing may react differently to a static magnetic field once an additional time-periodic field has been added. Thus, despite the formal similarity of our key results (106) and (107) to their historical antecessors (96) and (97), these former equations may have the potential to open up an altogether new line of research.

Acknowledgments

This work has been supported by the Deutsche Forschungsgemeinschaft (DFG, German Research Foundation) through Projects 355031190, 397122187 and 397300368. We thank all members of the Research Unit FOR 2692 for stimulating and insightful discussions.

Appendix A: Remarks on the lifting procedure

The technique of lifting a matrix solution of the time-dependent Schrödinger equation for $s = 1/2$ to general s , as reviewed briefly in Subsec. IIB, has been repeatedly used in this paper. In this Appendix we illustrate this

technique with the help of an elementary example from classical mechanics.

Consider the motion of a rigid body, and let \vec{r}_0 denote a constant position vector in a reference frame fixedly attached to that body (“B-system”). Then this vector is expressed by

$$\vec{r}(t) = B(t) \vec{r}_0 \quad (\text{A1})$$

with respect to some inertial laboratory system (“L-system”), where the rotational 3×3 -matrix $B(t)$ satisfies both $B(t)^\top = B(t)^{-1}$ and $\det B(t) = 1$. Differentiating Eq. (A1) with respect to time gives

$$\frac{d}{dt} \vec{r}(t) \equiv \dot{\vec{r}} = \dot{B} \vec{r}_0 = \left(\dot{B} B^\top \right) \vec{r}(t) \equiv \Omega(t) \vec{r}(t), \quad (\text{A2})$$

where the anti-symmetric real 3×3 -matrix

$$\Omega(t) = \dot{B}(t) B^\top(t) \quad (\text{A3})$$

has been introduced. This equation $\dot{\vec{r}} = \Omega(t) \vec{r}(t)$ is nothing but the matrix version of the familiar equation

$$\dot{\vec{r}} = \vec{\omega} \times \vec{r}, \quad (\text{A4})$$

involving the vector $\vec{\omega}$ of angular velocity in the L-system; this vector is constant for all points of the rigid body. Next, let $\vec{\ell}$ be the angular momentum of the rigid body in the L-system, implying that the corresponding vectors in the B-system are given by

$$\begin{aligned} \vec{\Omega} &= B(t)^\top \vec{\omega} \\ \vec{L} &= B(t)^\top \vec{\ell}. \end{aligned} \quad (\text{A5})$$

As is well known, the linear relation between $\vec{\Omega}$ and \vec{L} can be written as

$$\vec{L} = \Theta \vec{\Omega}, \quad (\text{A6})$$

where the time-independent, symmetric 3×3 -matrix Θ denotes the inertial tensor of the rigid body in the B-system. Exploiting Eqs. (A5), one obtains the corresponding inertial tensor $\theta(t)$ in the L-system,

$$\vec{\ell} = B \vec{L} = B \Theta \vec{\Omega} = (B \Theta B^\top) \vec{\omega} \equiv \theta(t) \vec{\omega}. \quad (\text{A7})$$

Utilizing $\dot{B} B^\top + B \dot{B}^\top = 0$ and, hence,

$$\dot{B}^\top = -B^\top \dot{B} B^\top = -B^\top \Omega, \quad (\text{A8})$$

its time derivative takes the form

$$\begin{aligned} \dot{\theta} &= \dot{B} \Theta B^\top + B \Theta \dot{B}^\top \\ &= \Omega B \Theta B^\top + B \Theta (-B^\top \Omega) = [\Omega, \theta], \end{aligned} \quad (\text{A9})$$

with the last bracket denoting the commutator of two 3×3 -matrices.

While this equation (A9) has been derived above in an elementary though somewhat tedious manner, we will

now show that it follows directly from Eq. (A3) by group-theoretical arguments.

To this end, we translate the above considerations into the appropriate group-theoretical language. Obviously, the matrices $B(t)$ connecting the B- and the L-system are elements of the Lie group $SO(3)$, and $\Omega(t)$ belongs to the associated Lie algebra $so(3)$ of real anti-symmetric 3×3 -matrices. Its defining equation (A3) then is recognized as an immediate analog of the matrix Schrödinger equation (22) which has served as starting point in Subsec. II B. Moreover, the transformation $\Theta \mapsto \theta = B \Theta B^\top$ implied by Eq. (A7) can be viewed as an operation of B on the space of symmetric 3×3 -matrices Θ , and hence as a 6-dimensional representation R of $SO(3)$:

$$\theta = R(B)(\Theta) = B \Theta B^\top. \quad (\text{A10})$$

It is not irreducible but can be split into 1- and 5-dimensional irreps due to the rotational invariance of the trace of Θ . The corresponding 6-dimensional representation r of the Lie algebra $so(3)$ is then given by

$$r(\Omega)(\Theta) = [\Omega, \Theta]. \quad (\text{A11})$$

This follows if B is written as $B = \mathbb{1} + \epsilon \Omega$ with an anti-symmetric 3×3 -matrix Ω , so that Eq. (A10) yields

$$\begin{aligned} R(\mathbb{1} + \epsilon \Omega)(\Theta) &= (\mathbb{1} + \epsilon \Omega) \Theta (\mathbb{1} - \epsilon \Omega) \\ &= \Theta + \epsilon [\Omega, \Theta] + O(\epsilon^2). \end{aligned} \quad (\text{A12})$$

Now the definition (A10) implies

$$\dot{\theta} = \left(\frac{d}{dt} R(B) \right) (\Theta) = \left(\frac{d}{dt} R(B) \right) R(B)^{-1}(\theta), \quad (\text{A13})$$

so that the above Eq. (A9) can be expressed in the form

$$\left(\frac{d}{dt} R(B) \right) R(B)^{-1}(\theta) = r(\Omega)(\theta). \quad (\text{A14})$$

This is the lifted image of Eq. (A3), in the same sense as the Schrödinger equation (29) in Subsec. II B is the lifted image of Eq. (22). Thus, it would have been possible to deduce Eq. (A9) immediately from Eq. (A3) in a single step.

Appendix B: Damped spin precession

Instead of a driven spin coupled to a heat bath, here we consider a classical unit spin vector $\mathbf{S}(t)$ under the influence of both a magnetic field $\mathbf{b}(t)$ conforming to Eq. (35) and a nonlinear damping mechanism satisfying an equation of the Landau-Lifshitz type [45],

$$\frac{d}{dt} \mathbf{S} = -\mathbf{S} \times \mathbf{b} + g \mathbf{S} \times (\mathbf{S} \times \mathbf{b}), \quad (\text{B1})$$

where the parameter $g > 0$ describes the strength of the damping. (Note that the unusual signs have been chosen

here because the spin vector of an electron points into the direction opposite to that of the magnetic moment.) Analogously to the elementary case of a classical damped, periodically driven oscillator it can be shown that asymptotically for $t \rightarrow \infty$ the solution of Eq. (B1) becomes a rotation about the \mathbf{b}_z -axis with the same frequency as the field $\mathbf{b}(t)$ and a constant phase shift,

$$\mathbf{S}(t) = \begin{pmatrix} \sqrt{1-z^2} \cos(\omega t - \phi) \\ \sqrt{1-z^2} \sin(\omega t - \phi) \\ z \end{pmatrix}. \quad (\text{B2})$$

The functions $z = z(\omega_0, \omega, F, g)$ and $\phi = \phi(\omega_0, \omega, F, g)$ can be determined analytically, but are too lengthy to be reproduced here. Let

$$E(t) = \mathbf{S}(t) \cdot \mathbf{b}(t) \quad (\text{B3})$$

be the energy of the spin in the field; this function $E(t)$ will be a periodic function of t for the special solution (B2). Differentiating, we find

$$\begin{aligned} \dot{E} &= \dot{\mathbf{S}} \cdot \mathbf{b} + \mathbf{S} \cdot \dot{\mathbf{b}} \\ &= -(\mathbf{S} \times \mathbf{b}) \cdot \mathbf{b} + g(\mathbf{S} \times (\mathbf{S} \times \mathbf{b})) \cdot \mathbf{b} + \mathbf{S} \cdot \dot{\mathbf{b}} \\ &= g((\mathbf{S} \cdot \mathbf{b})^2 - \mathbf{b}^2) + \mathbf{S} \cdot \dot{\mathbf{b}}. \end{aligned} \quad (\text{B4})$$

Integrating \dot{E} over one period gives 0, implying that the time averages of the final two terms in Eq. (B4) must cancel. It is plausible to regard the first term

$$q \equiv g((\mathbf{S} \cdot \mathbf{b})^2 - \mathbf{b}^2) \leq 0 \quad (\text{B5})$$

as the heat loss of the driven spin due to the damping, and the second term

$$w \equiv \mathbf{S} \cdot \dot{\mathbf{b}} \quad (\text{B6})$$

as the work performed on the spin by the driving field, so that the time average of w must be positive. A short calculation yields

$$w = |q| = -F \omega \sqrt{1-z^2} \sin \phi \quad (\text{B7})$$

which is independent of t , so that time-averaging is not necessary here. Note that $w \geq 0$ requires that the phase shift ϕ satisfies $\pi \leq \phi \leq 2\pi$. In Fig. 12 we have plotted $|q|$ as a function of ω/ω_0 for parameters taken from Fig. 10 and observe qualitative agreement with r_∞ as drawn therein, suggesting a close connection between the heat-bath model and the phenomenological Landau-Lifshitz equation (B1).

A thorough investigation of this connection would require knowledge of the relation between the dissipation constant g and the parameters of the heat-bath model. While a rigorous derivation of that relation is beyond the scope of this Appendix, one may obtain insight from a simple dimensional argument: Comparing the factors of dimension 1/time which set the scale for the relaxation

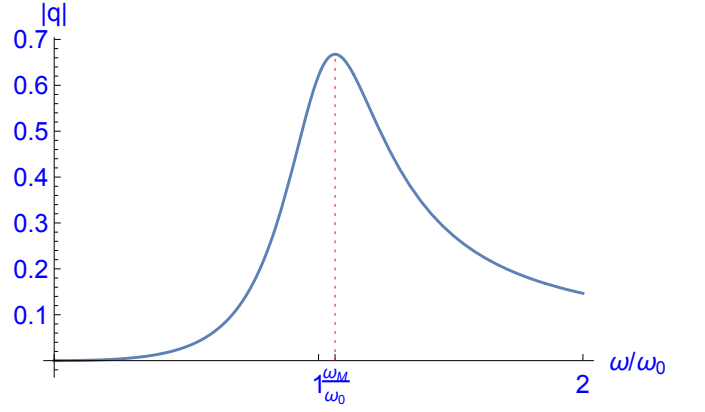


FIG. 12: (Color online) Absolute value of the dissipated heat $|q|$ of the classical damped, periodically driven spin described by the Landau-Lifshitz equation (B1) as a function of ω/ω_0 . Parameters are $F/\omega_0 = 1/4$, and $g = 0.1$.

rate implied by Eq. (B1) on the one hand, and for the rates (65) and (69) on the other, we deduce

$$g|\mathbf{b}| \sim \Gamma_0 = 2\pi\gamma^2 J_0, \quad (\text{B8})$$

where the symbol “ \sim ” is supposed to indicate “equality up to dimensionless numbers of order one”.

The rate $|q|$ of dissipated heat can then be expressed in two different ways. According to Eq. (B5), one has

$$|q| \sim g|\mathbf{b}|^2 = g(F^2 + \omega_0^2). \quad (\text{B9})$$

On the other hand, the maximum dimensionless scaled dissipation rate r_m in the classical limit $s \rightarrow \infty$ is given by Eq. (119), implying the estimate

$$\begin{aligned} R_m &= \omega_0 \Gamma_0 r_m \\ &\sim \Gamma_0 \left(\omega_0 + \sqrt{F^2 + \omega_0^2} \right) \\ &\sim g|\mathbf{b}| \left(\omega_0 + \sqrt{F^2 + \omega_0^2} \right) \\ &\sim g \left(F^2 + \omega_0^2 + \omega_0 \sqrt{F^2 + \omega_0^2} \right) \end{aligned} \quad (\text{B10})$$

for the full rate. This is compatible with the above relation (B9), again hinting at an intrinsic connection between the heat-bath model studied in the main text, and the Landau-Lifshitz equation (B1), so that the remarkable similarity between Figs. 10 and 12 is no coincidence.

-
- [1] Ya. B. Zel'dovich, *The quasienergy of a quantum-mechanical system subjected to a periodic action*, J. Exptl. Theoret. Phys. (U.S.S.R.) **51**, 1492 (1966) [Sov. Phys. JETP **24**, 1006 (1967)].
- [2] H. Sambe, *Steady states and quasienergies of a quantum-mechanical system in an oscillating field*, Phys. Rev. A **7**, 2203 (1973).
- [3] A. G. Fainshtein, N. L. Manakov, and L. P. Rapoport, *Some general properties of quasi-energetic spectra of quantum systems in classical monochromatic fields*, J. Phys. B: Atom. Molec. Phys. **11**, 2561 (1978).
- [4] R. Blümel, A. Buchleitner, R. Graham, L. Sirko, U. Smilansky, and H. Walther, *Dynamical localization in the microwave interaction of Rydberg atoms: The influence of noise*, Phys. Rev. A **44**, 4521 (1991).
- [5] M. Grifoni and P. Hänggi, *Driven quantum tunneling*, Phys. Rep. **304**, 229 (1998).
- [6] S. Gasparinetti, P. Solinas, S. Pugnetti, R. Fazio, and J. P. Pekola, *Environment-governed dynamics in driven quantum systems*, Phys. Rev. Lett. **110**, 150403 (2013).
- [7] T. M. Stace, A. C. Doherty, and D. J. Reilly, *Dynamical steady states in driven quantum systems*, Phys. Rev. Lett. **111**, 180602 (2013).
- [8] J. Zhang, P. W. Hess, A. Kyprianidis, P. Becker, A. Lee, J. Smith, G. Pagano, I.-D. Potirniche, A. C. Potter, A. Vishwanath, N. Y. Yao, and C. Monroe, *Observation of a discrete time crystal*, Nature **543**, 217 (2017).
- [9] S. Choi, J. Choi, R. Landig, G. Kucsko, H. Zhou, J. Isoya, F. Jelezko, S. Onoda, H. Sumiya, V. Khemani, C. von Keyserlingk, N. Y. Yao, E. Demler, and M. D. Lukin, *Observation of discrete time-crystalline order in a disordered dipolar many-body system*, Nature **543**, 221 (2017).
- [10] W. Kohn, *Periodic Thermodynamics*, J. Stat. Phys. **103**, 417 (2001).
- [11] H.-P. Breuer, W. Huber, and F. Petruccione, *Quasistationary distributions of dissipative nonlinear quantum oscillators in strong periodic driving fields*, Phys. Rev. E **61**, 4883 (2000).
- [12] R. Ketzmerick and W. Wustmann, *Statistical mechanics of Floquet systems with regular and chaotic states*, Phys. Rev. E **82**, 021114 (2010).
- [13] D. W. Hone, R. Ketzmerick, and W. Kohn, *Statistical mechanics of Floquet systems: The pervasive problem of near-degeneracies*, Phys. Rev. E **79**, 051129 (2009).
- [14] G. Bulnes Cuetara, A. Engel, and M. Esposito, *Stochastic thermodynamics of rapidly driven systems*, New J. Phys. **17**, 055002 (2015).
- [15] T. Shirai, T. Mori, and S. Miyashita, *Condition for emergence of the Floquet-Gibbs state in periodically driven open systems*, Phys. Rev. E **91**, 030101(R) (2015).
- [16] D. E. Liu, *Classification of the Floquet statistical distribution for time-periodic open systems*, Phys. Rev. B **91**, 144301 (2015).
- [17] T. Iadecola, and C. Chamon, *Floquet systems coupled to particle reservoirs*, Phys. Rev. B **91**, 184301 (2015).
- [18] T. Iadecola, T. Neupert, and C. Chamon, *Occupation of topological Floquet bands in open systems*, Phys. Rev. B **91**, 235133 (2015).
- [19] K. I. Seetharam, C.-E. Bardyn, N. H. Lindner, M. S. Rudner, and G. Refael, *Controlled population of Floquet-Bloch states via coupling to Bose and Fermi baths*, Phys. Rev. X **5**, 041050 (2015).
- [20] D. Vorberg, W. Wustmann, H. Schomerus, R. Ketzmerick, and A. Eckardt, *Nonequilibrium steady states of ideal bosonic and fermionic quantum gases*, Phys. Rev. E **92**, 062119 (2015).
- [21] S. Vajna, B. Horovitz, B. Dóra, and G. Zaránd, *Floquet topological phases coupled to environments and the induced photocurrent*, Phys. Rev. B **94**, 115145 (2016).
- [22] S. Restrepo, J. Cerrillo, V. M. Bastidas, D. G. Angelakis, and T. Brandes, *Driven open quantum systems and Floquet stroboscopic dynamics*, Phys. Rev. Lett. **117**, 250401 (2016).
- [23] A. Lazarides and R. Moessner, *Fate of a discrete time crystal in an open system*, Phys. Rev. B **95**, 195135 (2017).
- [24] K. I. Seetharam, C.-E. Bardyn, N. H. Lindner, M. S. Rudner, and G. Refael, *Steady states of interacting Floquet insulators*, Phys. Rev. B **99**, 014307 (2019).
- [25] I. I. Rabi, *Spin quantization in a gyrating magnetic field*, Phys. Rev. **51**, 652 (1937).
- [26] L. Brillouin, *Les moments de rotation et le magnétisme dans la mécanique ondulatoire*, J. Phys. Radium **8**, 74 (1927).
- [27] W. E. Henry, *Spin Paramagnetism of Cr^{+++} , Fe^{+++} , and Gd^{+++} at Liquid Helium Temperatures and in Strong Magnetic Fields*, Phys. Rev. **88**, 559 (1952).
- [28] R. H. Fowler and E. A. Guggenheim, *Statistical Thermodynamics* (Cambridge University Press, Cambridge, 1939).
- [29] For a modern exposition see, e.g., R. K. Pathria, *Statistical Mechanics* (Academic Press, New York; 3rd edition, 2011).
- [30] M. Langemeyer and M. Holthaus, *Energy flow in periodic thermodynamics*, Phys. Rev. E **89**, 012101 (2014).
- [31] H.-J. Schmidt, *The Floquet theory of the two-level system revisited*, Z. Naturforsch. A **73**, 705 (2018).
- [32] L. D. Landau and E. M. Lifshitz, *Quantum Mechanics: Non-Relativistic Theory*, § 57 (Butterworth-Heinemann, 3rd revised edition, reprinted 1981).
- [33] F. T. Hioe, *N-level quantum systems with $SU(2)$ dynamic symmetry*, J. Opt. Soc. Am. B **4**, 1327 (1987).
- [34] V. L. Pokrovsky and N. A. Sinitsyn, *Spin transitions in time-dependent regular and random magnetic fields*, Phys. Rev. B **69**, 104414 (2004).
- [35] See, e.g., B. C. Hall, *Lie Groups, Lie Algebras, and Representations: An Elementary Introduction*, Graduate Texts in Mathematics **222** (Springer, New York; 2nd edition, 2015).
- [36] M. Holthaus and B. Just, *Generalized π -pulses*, Phys. Rev. A **49**, 1950 (1994).
- [37] J. H. Shirley, *Solution of the Schrödinger equation with a Hamiltonian periodic in time*, Phys. Rev. **138**, B 979 (1965).
- [38] W. R. Salzman, *Quantum mechanics of systems periodic in time*, Phys. Rev. A **10**, 461 (1974).
- [39] F. Gesztesy and H. Mitter, *A note on quasi-periodic states*, J. Phys. A: Math. Gen. **14**, L79 (1981).
- [40] M. Holthaus, *Floquet engineering with quasienergy bands of periodically driven optical lattices*, J. Phys. B: At. Mol. Opt. Phys. **49**, 013001 (2016).

- [41] Note a minor deviation from Ref. [30], where $V = \gamma \sigma_x = 2\gamma s_x$.
- [42] O. R. Diermann, H. Frerichs, and M. Holthaus, *Periodic thermodynamics of the parametrically driven harmonic oscillator*, Phys. Rev. E **100**, 012102 (2019).
- [43] G. R. Eaton, S. S. Eaton, D. P. Barr, and R. T. Weber, *Quantitative EPR* (Springer-Verlag, Wien; 2010).
- [44] S. Gasparinetti, P. Solinas, A. Braggio, and M. Sassetti, *Heat-exchange statistics in driven open quantum systems*, New J. Phys. **16**, 115001 (2014).
- [45] L.D. Landau and E.M. Lifshitz, *Theory of the dispersion of magnetic permeability in ferromagnetic bodies*, Phys. Z. Sowjetunion **8**, 153 (1935).
- [46] K. Petukhov, W. Wernsdorfer, A.-L. Barra, and V. Mosser, *Resonant photon absorption in Fe₈ single-molecule magnets detected via magnetization measurements*, Phys. Rev. B **72**, 052401 (2005).